FISEVIER

Contents lists available at ScienceDirect

Quaternary Science Reviews

journal homepage: www.elsevier.com/locate/quascirev



Using sediment accumulation rates in floodplain paleochannel lakes to reconstruct climate-flood relationships on the lower Ohio River



Derek K. Gibson ^a, Broxton W. Bird ^{a, b, *}, Harvie J. Pollard ^{a, 1}, Cameron A. Nealy ^a, Robert C. Barr ^b, Jaime Escobar ^{c, d}

- ^a Department of Earth Sciences, Indiana University-Purdue University, Indianapolis (IUPUI), USA
- ^b Center for Earth and Environmental Sciences, IUPUI, USA
- ^c Department of Civil and Environmental Engineering, Universidad Del Norte, Colombia
- ^d Smithsonian Tropical Research Institute, Panama City, Panama

ARTICLE INFO

Article history: Received 12 July 2022 Received in revised form 8 October 2022 Accepted 30 October 2022 Available online xxx

Keywords:
Holocene
North America
Paleoclimatology
Sedimentology
Flooding
Fluvial geomorphology
Medieval climate anomaly
Little ice age

ABSTRACT

Late Holocene flood frequencies on the lower Ohio River were investigated using 14C-based sedimentation rates from three floodplain lakes located in Illinois (Avery Lake), Kentucky (Grassy Pond), and Indiana (Goose Pond). Changes in sediment accumulation rates were attributed to variability in the delivery of overbank sediment to each site as controlled by the frequency of Ohio River flooding. Sedimentation rates reached their lowest values in all three lakes between 400 and 1230 CE, indicating a regional reduction in flood frequencies on the lower Ohio River during a period that included the Medieval Climate Anomaly (MCA; ca. 950-1250 CE). Sedimentation rates increased after ca. 1230 CE and remained moderately high through the Little Ice Age (LIA; 1350-1820 CE) until the onset of extensive land clearance during the early 1800s CE. After 1820 CE, sedimentation rates increased further and were higher than any other time during the late Holocene. A comparison of regional paleoclimatic proxies with the above floodplain sedimentation records shows that Ohio River flooding during the late Holocene was responsive to mean-state changes in atmospheric circulation. During the MCA, when clockwise meanstate atmospheric circulation advected southerly moisture from the Gulf of Mexico into the Ohio River Valley primarily in the form of convective rainstorms, flooding on the Ohio River was least frequent. During the LIA, meridional mean-state atmospheric circulation increased the proportion of midcontinental moisture that was sourced from the northern Pacific and Arctic and delivered as snowfall, hence increasing flooding on the Ohio River. We attribute the increase in Ohio River flooding during the LIA to an increase in snowpack volume across the Ohio River Valley and the watershed-scale integration of runoff during spring snowmelt. Following Euro-American land clearance in the early 1800s, flood frequencies decoupled from this relationship and the lower Ohio River became susceptible to frequent flooding, despite a return to southerly and clockwise synoptic atmospheric conditions. These modern climate-flood dynamics are fundamentally different than those of the paleo-record and suggest that land-use changes – such as deforestation, tile draining, and landscape conversion to intensive row crop agriculture - have fundamentally altered the modern Midwestern hydrologic cycle.

© 2022 Elsevier Ltd. All rights reserved.

1. Introduction

The frequency of flood events in the Midwestern United States

has increased in recent decades (Mallakpour and Villarini, 2015) in response to a 15% increase in annual precipitation since 1980 and a 40% increase in extreme precipitation events since the late 1950s (Easterling et al., 2017). One consequence of this trend is that fluvial erosion and channel mobility have accelerated, impacting infrastructure, agricultural operations, and communities in proximity to fluvial systems, and, in many cases, resulting in damages that have ranged from millions to billions of dollars (Smith and Katz, 2013). Because the Midwest is one of the world's largest agricultural

^{*} Corresponding author. Department of Earth Sciences, Indiana University-Purdue University, Indianapolis (IUPUI), USA.

E-mail address: bwbird@iupui.edu (B.W. Bird).

¹ Currently with the United States Geological Survey, Ohio-Kentucky-Indiana Water Science Center

exporters and a global leader in corn, wheat, and soybean production and exportation, fluvial hazards in this region can additionally impact global food supply chains with severe economic consequences (Hatfield et al., 2012; Xiao et al., 2013; Mallakpour and Villarini, 2015). Future hydrologic outlooks for the Midwest suggest that annual precipitation may increase by an additional 20% by 2070, due primarily to wetter spring and winter seasons (Easterling et al., 2017), which is likely to further exacerbate fluvial hazards. To develop strategies for fluvial hazard mitigation and flood resilience, it is important to better understand how modern land-use has impacted the relationships between synoptic-scale climate dynamics and flood recurrence. To accomplish this task, it is first necessary to determine "natural," pre-industrial, climateflood relationships. However, long records that reflect linkages between natural mean-state atmospheric circulation, precipitation seasonality, and flood recurrence in the Midwest are sparse (Bird et al., 2019).

At present, the most destructive Midwestern flood events generally occur during the mid-to-late spring when precipitation is heaviest and watershed soils are saturated due to spring snowmelt (Kunkel et al., 1994; Andresen et al., 2012). Based on these observations, it has been hypothesized that pre-industrial flood recurrence during the late Holocene would have been most common when zonal mean-state atmospheric circulation over the Midwest produced clockwise atmospheric flow that advected warm, moist vapor masses from the Gulf of Mexico and increased spring and summer precipitation (Knox, 2000). However, a recent investigation of the long-term relationship between Midwestern climate and flooding suggested that flood recurrence on the lower Ohio River was most frequent during the Little Ice Age (LIA; 1350–1820 CE) – a period dominated by Pacific-sourced cold-season precipitation delivered by northerly atmospheric circulation - and comparatively infrequent during the Medieval Climate Anomaly (MCA; 950–1250 CE), when clockwise atmospheric circulation over the Midwest directed moisture from the Gulf of Mexico deep into the midcontinent (Bird et al., 2019).

One explanation for the differences between modern and preindustrial flood regimes may be that current fluvial dynamics are occurring within the context of a highly altered landscape. Since the early 1800s, widespread deforestation and the installation of tile drainage systems for agricultural operations have fundamentally altered the Midwestern hydrologic cycle by decreasing interception and infiltration and increasing runoff (Bonan, 1999; Greeley, 1925; King et al., 2014; Schilling and Helmers, 2008). As a result, the Ohio River may be more susceptible to flooding at present, despite southerly dominated atmospheric circulation and a predominance of spring and summer precipitation – conditions that were shown to reduce flooding during the pre-industrial past (Bird et al., 2019). However, because very few instrumental records exist prior to the 1800s and regional paleoclimate proxies that represent climateflood relationships are sparse, it is difficult to establish how large fluvial systems like the Ohio River responded in the past to meanstate hydroclimatic changes. Despite these challenges, determining how the frequency of flood events has varied through time in response to changing climatic and land use conditions has important implications for models of flood recurrence and landscape evolution over a range of timescales.

To examine climate-flood relationships prior to instrumental record-keeping and test the hypothesis that modern land use has impacted flood patterns on the Ohio River, long proxy records of climate and fluvial responses are needed. Sediments preserved in floodplain lakes provide one such archive of paleo-fluvial processes, including flood frequency and floodplain development (e.g., Munoz et al., 2015; Lintern et al., 2016; Bird et al., 2019). Oxbow lakes and other paleochannels situated in floodplains adjacent to

modern fluvial systems are inundated with sediment-laden flood-waters during high-discharge events (Constantine et al., 2010). Constraining variability in sediment accumulation rates at these sites can therefore be used to reconstruct changes in frequencies of discharges capable of inundating these sites through time. Such records can provide a unique perspective of how fluvial systems and their floodplains functioned under pre-industrial conditions and capture the consequences of modern land use and climate change on fluvial dynamics (e.g., Bird et al., 2019).

Here, we present new sediment accumulation rate records from two floodplain lakes located along the lower Ohio River in northern Kentucky and southern Indiana and synthesize these results with the only presently published Ohio River paleo-flood record from Avery Lake, Illinois (Bird et al., 2019). Variability in sediment accumulation rates, chronologically constrained by ¹⁴C and industrial Pb pollution, are used as a proxy for flood frequency over the past ca. 1900 years and compared to high resolution, multi-proxy climate records from the Midwest that span the same period to investigate the pre-industrial relationships between Midwestern climate (e.g., temperature, precipitation source, and atmospheric circulation) and flood recurrence on the Ohio River.

2. Regional setting

2.1. Floodplain sedimentation and morphometry in the lower Ohio River Valley

The formation and evolution of floodplains and floodplain lakes are related to fluvial (in channel) and alluvial (out of channel) processes, which drive lateral and vertical floodplain dynamics. Overland runoff and bank erosion by meandering rivers provide suspended and bedload sediment, most of which is carried a short distance downstream and deposited as point, lateral, or midchannel bars (Lauer and Parker, 2008). When overbank flows occur, sediments are transported from the river channel onto the adjacent floodplain (Alexander and Prior, 1971; Wolman and Leopold, 1957), with coarse grained sediments deposited in close proximity to the main fluvial channel and fines (e.g., clays and silts) distributed more broadly across the floodplain. Significant accumulations of alluvial sediment can occur in closed depressions, i.e., floodplain lakes and swales created by abandoned stream channels, resulting in substantially higher sedimentation rates in these depositional environments compared to the floodplain at large (Asselman and Middelkoop, 1995; Lauer and Parker, 2008; Wolman and Leopold, 1957). Floodplain lakes typically have small, low-gradient, local watersheds, with limited or no permanent inflows. These characteristics limit the potential volume and mechanisms of sediment transport to these lakes when the adjacent river is below overbank discharge. At flood stage, however, the watersheds of floodplain lakes effectively become that of the adjacent river, providing a mechanism for sediment delivery and increasing the volume of sediment available (Toonen et al., 2012). As a result, alluvial sediments deposited during flood events often represent the vast majority, if not all, of the preserved sedimentary record in floodplain lakes (Citterio and Piégay, 2009; Fisk, 1947; Toonen et al., 2012). Consequently, variability in sediment accumulation rates in floodplain lakes are primarily driven by changes in the frequency of overbank flood events. Constraining sedimentation rates with high-resolution age modeling therefore provides estimates of the frequency of flood-related overbank sedimentation over time. Specifically, periods of high sedimentation rates in floodplain lakes can be interpreted to reflect greater overbank sedimentation as a result of more frequent flood events and vice versa for low sedimentation rates (e.g., Bird et al., 2019; Pollard, 2020; Wright, 2022).

The floodplain lakes used in this study to reconstruct Ohio River

flooding are located in the lower Ohio River watershed, in a ~2000 km² alluvial valley spanning southwestern Indiana, northwestern Kentucky, and southern Illinois (Fig. 1). The Ohio River is less bedrock constricted along this reach compared to other sections further upstream, which has allowed greater stream channel mobility in response to changes in discharge and sediment load during the late Glacial and Holocene (Counts et al., 2015). As a result, geomorphic features typical of a meandering stream system have formed along many reaches of the lower Ohio River, including terraces and point bars with ridge and swale topography (Alexander and Prior, 1971; Counts et al., 2015). All three lakes used in this study occupy the youngest of these terraces, which began forming approximately 4000 years ago (Counts et al., 2015).

2.2. Goose Pond, Indiana, and Grassy Pond, Kentucky

Goose Pond (37.9068° N, 87.8384° W; 105.7 m above sea level) is a small (0.05 km²) swale lake located on the southern tip of a moderately sized point bar (approx. 18.4 km²) along the lower Ohio River in southwestern Indiana, about 20 km upstream of its confluence with the Wabash River (Fig. 1). The floodplain is characterized by ridge and swale topography, with the topographic lows, or swales (including Goose Pond), interpreted as paleochannels and the topographic highs as natural levees left behind by the ancestral Ohio River as it built out to the southwest

(Alexander and Prior, 1971). Goose Pond is situated only 1.5 m above the main channel of the adjacent Ohio River (104.2 m above sea level) and is thus regularly inundated with water and sediment from the river during even low magnitude flood events (Fig. 1; Pollard, 2020).

Grassy Pond (37.8915° N, 87.9037° W; 105.3 m above sea level) is a small (0.25 km² — approximately 1.7 km \times 0.18 km) swale lake located on the northern tip of a point bar on the Kentucky side of the lower Ohio River, 14 km upstream of its confluence with the Wabash River (Fig. 1). Similar to the floodplain at Goose Pond, the ~35 km² Grassy Pond point bar is characterized by ridge and swale topography that was created as the Ohio River migrated westward. Grassy Pond is < 1 m above the main Ohio River channel (104.5 m above sea level), and so is regularly inundated during even low magnitude flood events, similar to Goose Pond.

At present, floodwaters from the Ohio River submerge Goose and Grassy ponds when discharges recorded at the Uniontown, KY stream gage exceed 11,215 cubic meters per second (cms), which corresponds to a water height of approximately 106 m above sea level (U.S. Geological Survey, 2020).

2.3. Avery Lake, Illinois

Avery Lake (37.0788 N, 88.4906 W; 96 m above sea level) is a small (0.13 km^2) swale lake located on an 80 km^2 floodplain on the

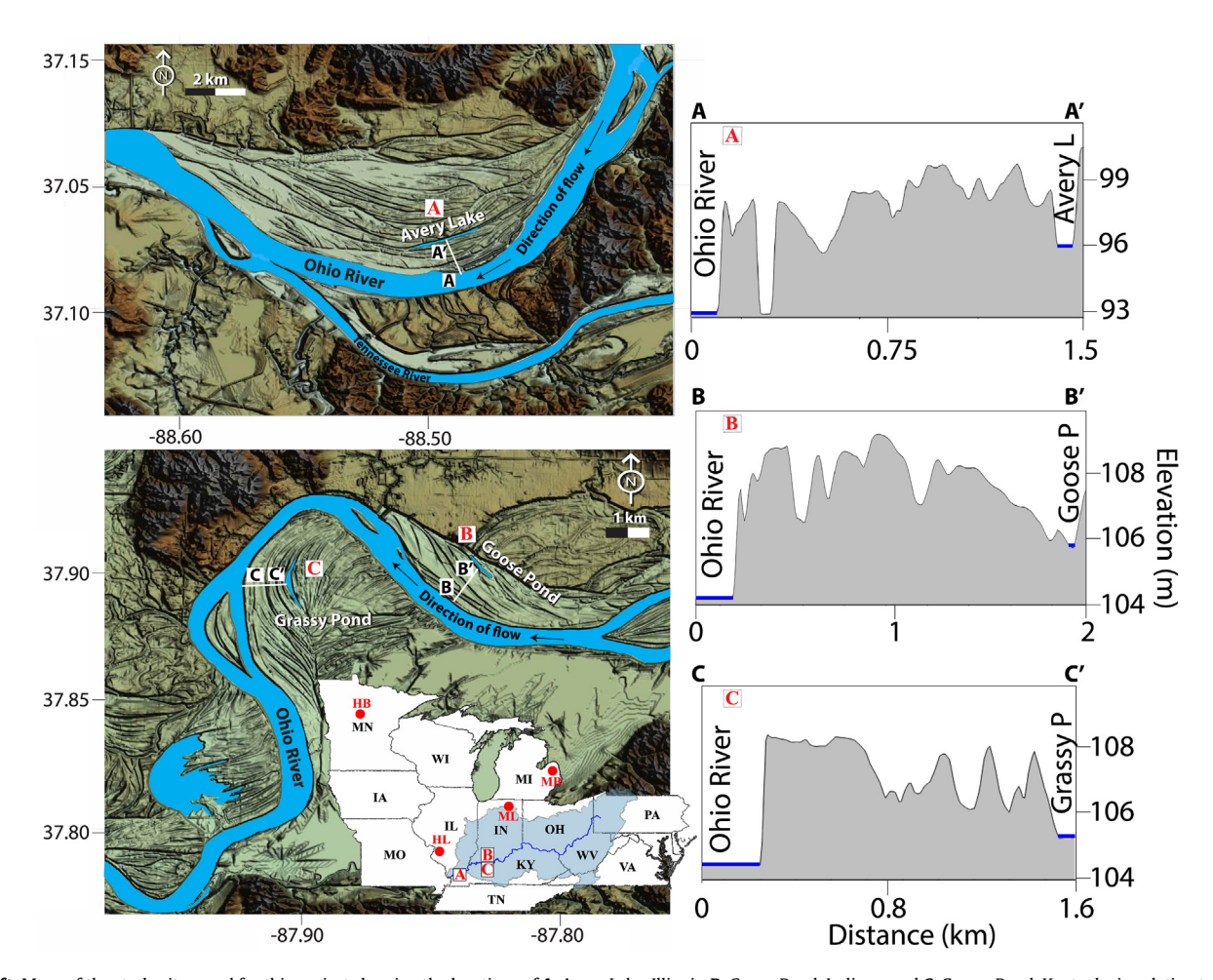


Fig. 1. Left: Maps of the study sites used for this project showing the locations of **A**. Avery Lake, Illinois, **B**. Goose Pond, Indiana, and **C**. Grassy Pond, Kentucky in relation to the Ohio River and its watershed (highlighted in blue). Isotope data and other paleoclimate proxies used for this study were sourced from Martin Lake, Indiana (ML; Bird et al., 2017), Minden and Hole Bogs, MI (MB & HB; Booth et al., 2006), and Horseshoe Lake, IL (HL; Pompeani et al., 2021). **Right:** Elevation profiles show floodplain topography and distances between **A**. Avery Lake, **B**. Goose Pond, and **C**. Grassy Pond and the modern Ohio River.

lower Ohio River in southeastern Illinois (Fig. 1 A). The Avery Lake floodplain is a meander loop-point bar system, which formed as the Ohio River migrated to the south over the past 10,000 to 20,000 years (Alexander and Nunnally, 1972; Alexander and Prior, 1968). Similar to the Goose and Grassy pond floodplains, the topography surrounding Avery Lake is characterized by ridges and swales created by the meander scars left behind as the Ohio River migrated (Alexander and Nunnally, 1972). The Avery Lake floodplain has an airfoil-like morphometry, with high elevations to the south and east (upstream) and lower elevations to the west and north. Avery Lake is situated on the elevated southern portion of the point bar ca. 3 m above the modern Ohio River. These topographic features result in a specific pattern of flooding that differs from flooding at Goose and Grassy ponds, whereby floodwaters inundate the Avery Lake floodplain first from the western, downstream, side of the point bar and slowly backfill, eventually overtopping the floodplain if discharges are sufficiently high (Alexander and Prior, 1971). The occurrence of low elevations on the northern portion of the floodplain further directs the highest velocity discharges away from the southern portion of the point bar where Avery Lake is located, resulting in low energy slack water deposits on the southern, higher-elevation portion of the point bar and at Avery Lake (Alexander and Prior, 1971).

The soil orders present across the Avery Lake point bar suggest that the aforementioned pattern of flooding was the long-term mean state at Avery Lake. High discharge velocities during flood events regularly scour and erode the soils to the north and west of Avery Lake, resulting in a predominance of immature inceptisols and entisols across this section of the floodplain. On the high elevation southern and eastern sections of the point bar, mature mollisols have developed, indicating that low energy slack water flooding, which lacks the necessary energy to regularly erode the soil, is common on the portion of the floodplain surrounding Avery Lake (ISEE Network, 2022).

In addition to differences in floodplain morphometry between Goose and Grassy ponds and Avery Lake, Avery Lake also has a long history of human occupation and land use, which impacted local erosion and runoff (and thus possibly influenced sedimentation rates in Avery Lake). Three major periods of pre-European occupation at Avery Lake have been identified in the archaeological record: The Baumer (600 BCE — 400 CE; Lapham, 2010), Lewis (600—900 CE; Pursell, 2016), and Mississippian phases. Of those, the Mississippian phase is the most recent (1000—1600 CE; Kessler et al., 2022) and is associated with large earthwork mounds, the adoption of maize agriculture, and the construction of extensive fortifications (Butler et al., 2011). In contrast, there is no evidence for large-scale pre-European occupation at either Goose or Grassy ponds during the periods represented by their sedimentary archives.

2.4. Modern climatology and streamflow in the Ohio River watershed

The modern climate of the Ohio River Valley is temperate, with minimum average temperatures ($-13\,^{\circ}\text{C}$) recorded in the Appalachian Plateau in January and maximum average temperatures (31 °C) occurring in southern Illinois and Indiana in July. Average annual precipitation across the Ohio River Valley ranges from 85 cm yr $^{-1}$ in the west to 150 cm yr $^{-1}$ in the east, with heavy and frequent precipitation events between April and June (Huang et al., 2021) from southerly- and southwesterly-sourced convective rainstorms (Dirmeyer and Kinter, 2010). Between December and February, precipitation is reduced and generally delivered as snow from cool, high-latitude frontal systems sourced from the northern Pacific and Arctic (Serreze et al., 1998).

The Pacific-North American teleconnection (PNA) is the main determinant of climatic conditions affecting the seasonal distribution and phase of precipitation across most of the midwestern and eastern United States - especially in the Ohio River Valley, where the correlation between PNA mode and precipitation is strongest for the continental US (Coleman and Rogers, 2003; Leathers et al., 1991: Liu et al., 2014). Positive phases of the PNA (+PNA) are associated with enhanced ridge and trough atmospheric circulation at the 500 hPa level that increases the frequency of midtropospheric air mass incursions from the Pacific Northwest. This pattern blocks moisture delivery from the Gulf of Mexico to the Midwestern United States, reducing overall precipitation in the Ohio and Mississippi River valleys (Archambault et al., 2008). Despite reduced precipitation during +PNA phases, the strong 500hPa trough and lower temperatures during precipitation events increases snowfall delivery to the Midwest and eastern United States such that the highest snowfall totals are often associated with +PNA phases (Serreze et al., 1998). Negative PNA phases (-PNA) are associated with more zonal midlatitude 500-hPa atmospheric flowpaths and a general increase in Midwestern precipitation, especially rainfall (Coleman and Rogers, 2003). This is due in part to a semi-stationary low-amplitude ridge situated over the US East Coast that steers Atlantic moisture and converges it into the Ohio River Valley (Nakamura et al., 2013). These conditions increase moisture advection from the Gulf of Mexico into the midcontinental US, which fuels convective rain events during the boreal summer (Leathers et al., 1991; Zhang and Villarini, 2019). While southerly and clockwise atmospheric circulation is more common during the summer, the occurrence of more extreme precipitation events related to atmospheric rivers, and other anomalous circulation events sourced from the Gulf of Mexico increase during all seasons under -PNA conditions (Lavers and Villarini, 2013; Nakamura et al., 2013). For example, zonal atmospheric flow, similar to -PNA conditions, are associated with increased average boreal winter discharge in the Ohio River and its tributaries (Rogers and Coleman, 2003).

Interannual temperature and precipitation fluctuations across the Ohio River Valley are strongly influenced by Pacific sea-surface temperature (SST) variability associated with the El Niño-Southern Oscillation (ENSO) (Hu and Feng, 2001; Birk et al., 2010). In the Midwest, warm ENSO phases (positive; +ENSO; El Niño events) are associated with warmer average temperatures and an overall decrease in precipitation and subsequent stream discharge across the region (Gershunov and Barnett, 1998; Rogers and Coleman, 2003). Conversely, cool (negative; -ENSO; La Niña) phases are associated with increased variability in near-surface temperature, an overall increase in precipitation (Andresen et al., 2012), and generally higher discharge in low-order tributaries (Singh et al., 2021). ENSO influences the phase of the PNA pattern such that they often occur in the same sign (i.e., both positive or both negative), which intensifies their hydroclimatic impacts (Yu and Zwiers, 2007; Henderson et al., 2020). When both teleconnections are in their positive mode, winter precipitation is considerably enhanced and the Ohio River Valley experiences a deep snowpack (Kluver and Leathers, 2015). When both teleconnections are in their negative mode, Midwestern precipitation and streamflow in Ohio River tributaries increase (Rogers and Coleman, 2003).

On decadal and longer timescales, precipitation across the Ohio River Valley is influenced by North Pacific SST variability associated with the Pacific Decadal Oscillation (PDO) (Mantua et al., 1997; Birk et al., 2010). Resembling + ENSO conditions, positive PDO phases (+PDO) are associated with warmer temperatures, less precipitation, and reduced stream discharge over the Ohio River Valley (Singh et al., 2021). Atmospheric circulation under these conditions resembles the +PNA, with a predominance of northwesterly

atmospheric flow from the northern Pacific and Arctic (Yu et al., 2007; Yu and Zwiers, 2007). Negative PDO (-PDO) phases are conversely similar to -ESNO conditions, with generally wetter conditions over the Ohio River Valley (Singh et al., 2021), though the relationship between the PDO, precipitation, and streamflow is generally weaker (Dai, 2013). Under -PDO conditions, mean-state atmospheric flow is more zonal and sourced from southerly sources (i.e., the Gulf of Mexico). While precipitation in the Ohio River Valley generally responds less strongly to PDO variability alone, the combined effects of ENSO and PDO can result in significant amplification when the mechanisms are in phase with one another, particularly when both are in their warm mode (Birk et al., 2010).

2.5. Modern hydrology and flood patterns of the Ohio River

The Ohio River is a large 8th-order stream (Horton, 1945; Strahler, 1957) with a watershed that encompasses approximately 420,000 km² (Schilling et al., 2015). This includes portions of 7 states across the eastern US (Pennsylvania, West Virginia, North Carolina, Ohio, Kentucky, Indiana, and Illinois) that are home to more than 25 million people (Fig. 1).

Stream gage data from four USGS monitoring stations (located at Sewickley, PA; Louisville, KY; Evansville, IN; and Metropolis, IL) that span the upper and lower Ohio River show that high discharge events (i.e., > the 1.5-year recurrence interval (RI) discharge) occur across the Ohio River Valley with similar seasonal timing. These gages were chosen due to their proximity to Avery Lake (Metropolis) and Goose and Grassy ponds (Evansville), and their distribution across the middle and upper Ohio River (Louisville and Sewickley, respectively). High and statistically signficant correlations between the number of high discharge events per month recorded at the Metropolis monitoring station and at the gages located at Evansville, Louisville, and Sewickley ($r^2 = 0.97, 0.97,$ and 0.88, respectively; p < 0.001) illustrate that high discharge events on the upper and lower Ohio River laregly occur during the early spring between March and April (Fig. 2; Table 1). This is consistent with large river systems in temperate climates where snowmelt and/or rain on snow events during the early spring are the primary driver of high discharge events rather than rainfall alone (Knox, 2000). This is because water from multiple precipitation events is stored as snowpack across the entire watershed and released essentially simultaneously during the spring melt. While locally important, rainstorms are simply not large enough to encompass a watershed the size of the Ohio River Valley and they deliver far less water per event relative to a winter's worth of snowpack. Consequently, variations in winter snowpack volumes are the primary driver of high discharge events on large rivers like the Ohio River (e.g., Graybeal and Leathers, 2006).

Due to the relationships between synoptic-scale atmospheric circulation and Ohio River Valley snowpack described above, mean-state conditions characterized by strong ridge and trough structure at the 500 hPa level and northerly atmospheric flow over the Midwest (i.e., +PNA) can increase winter snowpack and subsequent flood frequency, especially when amplified through constructive ENSO feedbacks (Birk et al., 2010; Singh et al., 2021). These modern relationships therefore provide a framework for better understanding past relationships between atmospheric circulation and Ohio River flood frequencies through time.

3. Methods

3.1. Sediment core retrieval

Sediment cores from Goose and Grassy Pond were collected using a modified Livingstone piston corer (Livingstone, 1955;

Wright et al., 1984) driven by a solar-powered electric winch mounted on a floating platform during the summer and fall of 2019. The cores were retrieved in sequential 1-m sections from adjacent holes with starting depths staggered by 50 cm to ensure that any sediment lost between core sections in one set of cores was captured in the other. Coring continued until refusal, which occurred after the sediments transitioned to coarse sand deposits that are consistent with modern lower Ohio River fluvial sediments (Alexander and Prior, 1971). The uppermost ~80 cm of each sediment core was captured using a modified piston corer with a ca. 7 cm diameter polycarbonate core barrel specifically designed to retrieve the undisturbed sediment-water interface (Fisher et al., 1992).

At Goose Pond, a composite 994 cm core was constructed from the Livingstone and surface cores by visually matching stratigraphic units and comparing magnetic susceptibility trends. Similar methods were used to retrieve and construct a 960 cm composite core from Grassy Pond.

3.2. X-ray fluorescence spectroscopy

X-ray fluorescence spectroscopy (XRF) is a quantitative analytical technique useful for estimating the elemental composition and abundance of geologic material, including sediments (Jenkins, 1999; de Vries and Vrebos, 2002). An Olympus Innov-X Delta Pro (DPO-6000-C) XRF spectrometer was used to quantify stratigraphic changes in the elemental composition of the sediments in the Goose Pond, Grassy Pond, and Avery Lake sediment cores (at 1 cm resolution for the Avery record and at 2-cm resolution for Goose and Grassy ponds). Two energy beams (40 kV and 10 kV; 30 s measurements for each beam) were used to measure the elemental composition of the lacustrine sediments, including sedimentary metal concentrations of Al, Si, Pb, and Zr. Elemental values were converted from counts per second to percent abundance using an Olympus calibration standard and proprietary software.

3.3. Age control

Age control for the sediment cores was provided primarily by radiocarbon accelerator mass spectroscopy (AMS ¹⁴C) of organic material preserved in the lake sediments. Organic samples were removed from the sediment cores, disaggregated with 7% H₂O₂, and sieved at 63 µm. Terrestrial organics - primarily charcoal, sticks, and leaves – were isolated and removed from the $>63 \mu m$ fraction. All samples were physically cleaned and chemically pre-treated following the University of California Irvine's Acid-Base-Acid protocol with 1 N HCl (at 70 °C) to remove any carbonate material, 1 N NaOH (at 70 °C) to remove organic acids, and a final 1 N HCl rinse (at 70 °C) to remove atmospheric carbon that may have accumulated during the alkaline wash (Olsson, 1986; Abbott and Stafford, 1996). All samples were then rinsed with 18-m Ω deionized water until they registered a neutral pH. The pretreated samples were sent to the University of California-Irvine, where they were combusted into CO2 gas, reduced to solid graphite, and analyzed for $^{14}\text{C}/^{13}\text{C}/^{12}\text{C}$ via AMS at the Keck-CCAMS facility.

An age model was created using the RStudio Bchron package, which calibrated the radiocarbon ages using the IntCal-20 calibration curve (Reimer et al., 2020), assigned error estimates and 1- σ confidence intervals, and plotted the calibrated age-depth relationships. Sedimentation rates for each lake were calculated using the Bchron acc_rate function, which provided minimum (25th percentile), maximum (75th percentile), and median (50th percentile) accumulation rate estimates based on the Bchron age models (Haslett and Parnell, 2008).

At Grassy Pond, the modern peak in anthropogenic Pb pollution

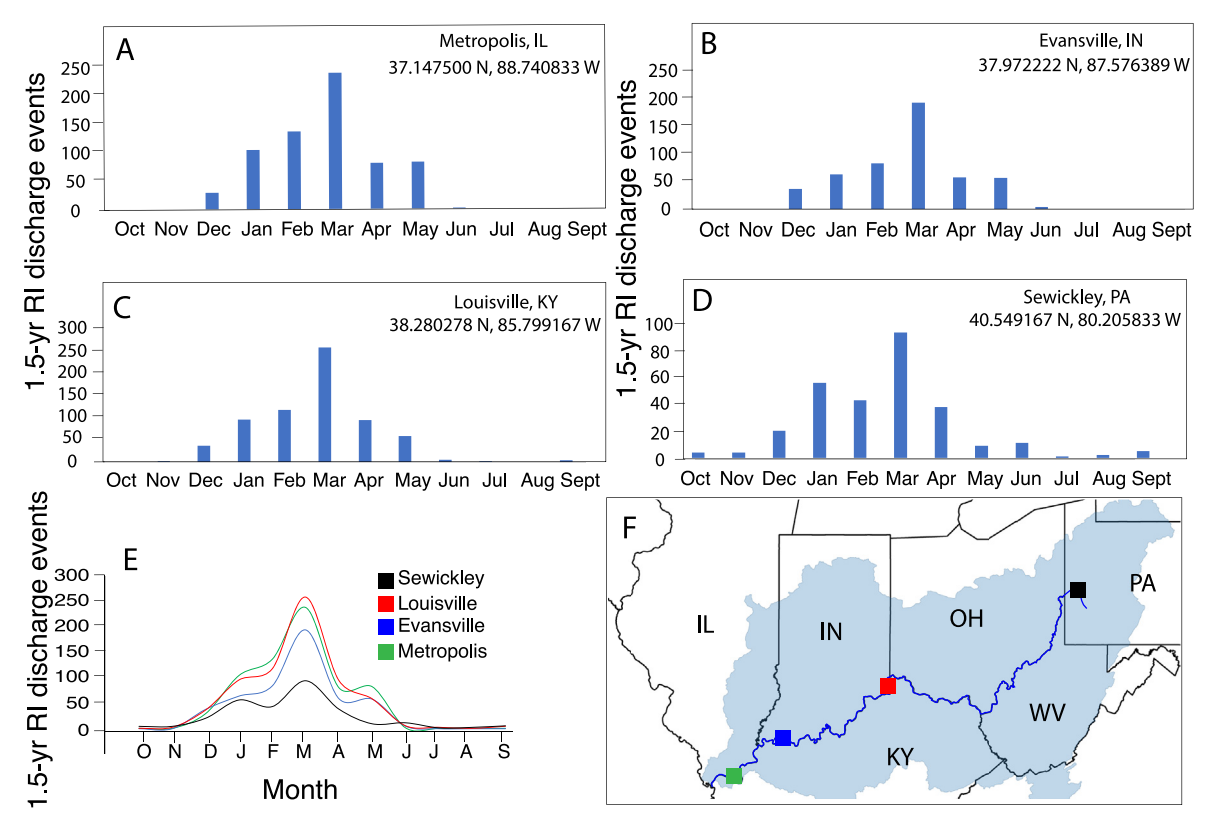


Fig. 2. Modern stream gage data showing the monthly distribution of flood events on the Ohio River from monitoring stations on the lower (A & B), middle (C), and upper (D) Ohio River. At present, flooding on the lower and upper Ohio River occurs in phase during the early spring (E) due to the watershed-scale integration of snowmelt. Panel F shows the locations of the monitoring stations in relation to the Ohio River watershed.

Table 1Regression of high discharge events (≥1.5-year recurrence interval) from USGS monitoring stations upstream of Avery Lake against discharge data from the Metropolis, IL stream gage station show that the timing of bankfull-or-greater discharge events occur across the upper and lower Ohio River with similar timing.

Gage Station	Latitude N	Longitude W	Coeff. Determ.	Corr. Coeff.	P Value
Sewickley, PA	40.549167	80.205833	0.8846	0.9405	< 0.00001
Louisville, KY	38.280278	85.799167	0.974	0.9869	< 0.00001
Evansville, IN	37.972222	87.576389	0.9708	0.9853	< 0.00001

was determined by normalizing XRF Pb abundances to the conservative terrestrial element Zr (e.g., (Boës et al., 2011). The resulting Pb/Zr peak that occurred at a depth of 170 cm was used as an additional age control anchor point for the year 1850 (± 20 years). This date corresponds with the timing of European settlement and industrialization of nearby Evansville, Indiana. European urbanization of the region began in the 1830s CE, and extensive coal mining operations and manufactured gas production were underway by the 1850s CE (Higgins and Higgins, 2019). Therefore, dating the anthropogenic Pb peak at 1850 CE and assigning a potential 40year range (from 1830 to 1870 CE) reasonably accounts for potential Pb pollution during the early settlement of the region during the 1830s CE, Pb pollution that was introduced due to the initial industrialization of Evansville during the 1850s CE, and a potential temporal lag between when the anthropogenic Pb was produced and when it entered the stream systems due to the time required for soil erosion and sediment transport to occur.

3.4. Grain size

Variability in the relative fractions of clay, silt, and sand in the Goose and Grassy pond cores was determined at 10-cm intervals to

investigate changes in depositional energy that occurred at each site as the distance and angle between the lakes and the main channel of the Ohio River changed through the late Holocene. For each sample, approximately 1 cm 3 of sediment was oxidized with concentrated (35%) $\rm H_2O_2$ to remove organics. The samples remained in the $\rm H_2O_2$ until the reaction ceased, then the $\rm H_2O_2$ was evaporated at 70 °C. The dried samples were then reconstituted with deionized water and mixed with 2 mL of dispersant (sodium metaphosphate; $\rm NaO_3P$). After this pretreatment, the samples were analyzed for grain size via laser diffraction at IUPUI using a Malvern Mastersizer 2000.

In addition to direct grain size measurements, granulometric proxies were used to infer stratigraphic changes in depositional energy represented in the sediment cores. A Geotek multi-sensor core logger was used to measure magnetic susceptibility on the Goose and Grassy pond cores at a 0.5 cm resolution after the cores had been left at room temperature for 24 h. In lacustrine sediments, magnetic minerals are primarily allochthonous and transported to the lake from the surrounding watershed and, in general, magnetic susceptibility has been demonstrated in various environmental settings to vary in-phase with grain size (Yim et al., 2004; Ghilardi et al., 2008). At Goose and Grassy ponds, we interpret increases in

magnetic susceptibility to reflect increases in the amount of coarsegrained terrestrial material delivered to the lake during flood events of the Ohio River. Similarly, variability in the ratio of Si to Al in the Goose and Grassy pond sediment cores was interpreted to reflect changes in the sand fraction of the sediments, delivered to the floodplain lakes by the Ohio River during flood events (e.g., Bouchez et al., 2011; Jonathan et al., 2004; Leigh, 2018).

3.5. Elemental abundance and isotopic composition of organic carbon and total nitrogen

The elemental abundance and isotopic composition of organic carbon (C) and total nitrogen (N) were determined at a 10-cm resolution from the Goose and Grassy pond cores at the University of Florida via a Carlo Erba NA 1500 CNS elemental analyzer connected to a Thermo Electron Delta V Advantage isotope ratio mass spectrometer with a ConFlo II interface. Approximately 10 mg of unacidified freeze-dried sample was weighed into tin capsules prior to isotopic analysis. Isotopic data are presented in terms of delta notation per mil (%), normalized to USGS 40 and USGS 41 A standard reference materials. Analytical precision for isotopic analysis was $\pm 0.10\%$ for C and $\pm 0.12\%$ for N. After processing, these results were compared to previously published nitrogen isotope data from Avery Lake (Bird et al., 2019) in order to examine differences in pre-European anthropogenic impacts between Avery Lake, which supported a large pre-European population, and Goose and Grassy ponds, which did not.

3.6. Modern stream gage data

Annual peak-flow discharge data that spanned the period from 1940 to 2019 were compiled from monitoring stations located on the lower and upper Ohio River at Metropolis, IL; Evansville, IN; Louisville, KY; and Sewickley, PA. These discharge data were recorded in cubic feet per second (\mathbf{f}^3/\mathbf{s}) by the USGS and converted to cubic meters per second (\mathbf{m}^3/\mathbf{s}) for the consistent presentation of units in this study. To calculate discharge recurrence intervals, annual peak flow data from each gage was sorted in descending order and ranked from highest discharge to lowest. Recurrence intervals were then calculated using the formula

$$RI = (N_y + 1)/N_r$$

where RI is the discharge recurrence interval, N_y is the number of years of recorded data, and N_r is the rank of each event. For this study, the 1.5-year recurrence interval was used as an estimation for bankfull discharge because it has been shown that this approximately corresponds to the lowest flood stage when effective discharge is highest in the Midwestern US (Leopold, 1994; Dunne and Leopold, 1978; Robinson, 2013).

4. Results

4.1. Sediment core stratigraphy

The bottom 24 cm of the Goose Pond core were characterized by medium-to-coarse grained sands that are consistent with the fluvial sedimentology of the modern and late Holocene Ohio River channel deposits (Alexander and Prior, 1971; Stafford and Creasman, 2002; Bird et al., 2019). From 970 to 810 cm, the sediments were homogenous, buff-to-tan colored (10 YR 8/8 to 10 YR 6/8), silt-to-clay sized (0.06–62 μ m; Wentworth, 1922), and contained very little macroscopic plant material. Between 810 and 560 cm, laminations, alternating dark and light colorations, and a slight increase in plant material characterized the sediments, which

were primarily silt-sized. Macroscopic organics continued to increase between 560 cm and 270 cm, including the presence of charcoal and terrestrial plant material. In this section, the sediments remained silt-to-clay sized and the color transitioned to brown (10 YR 4/6). The upper 270 cm of sediments were characterized by homogenous, tan (10 YR 6/8), silt-to-clay sized sediment that contained little macroscopic organic debris (Fig. 3).

The 960-cm-long Grassy Pond sediment core (Fig. 3 C & D) was divided into three sections based on visual stratigraphy. Between 960 and 900 cm, the core consisted of sand intermixed with woody plant debris, consistent with fluvial sediments deposited when the Grassy Pond swale was the active channel of the Ohio River. Between 874 and 792.5 cm, the sediments were predominantly silt-sized and contained large amounts of organic material, including terrestrial leaves and sticks. The uppermost and longest section, between 792 and 0 cm, consisted primarily of silts and clays consistent with low energy deposition characteristic of a lacustrine environment or overbank, slack water alluvial deposits (Fig. 3) (see Fig. 8).

4.2. Geochronology and sedimentation rates

20 AMS 14 C dates that span the last ~1900 years were used to construct the Goose Pond age model (Fig. 4 A; Table 2). High sedimentation rates (1.4 cm yr $^{-1}$) occurred immediately after the formation of Goose Pond at ca. 100 CE and remained high until ca.

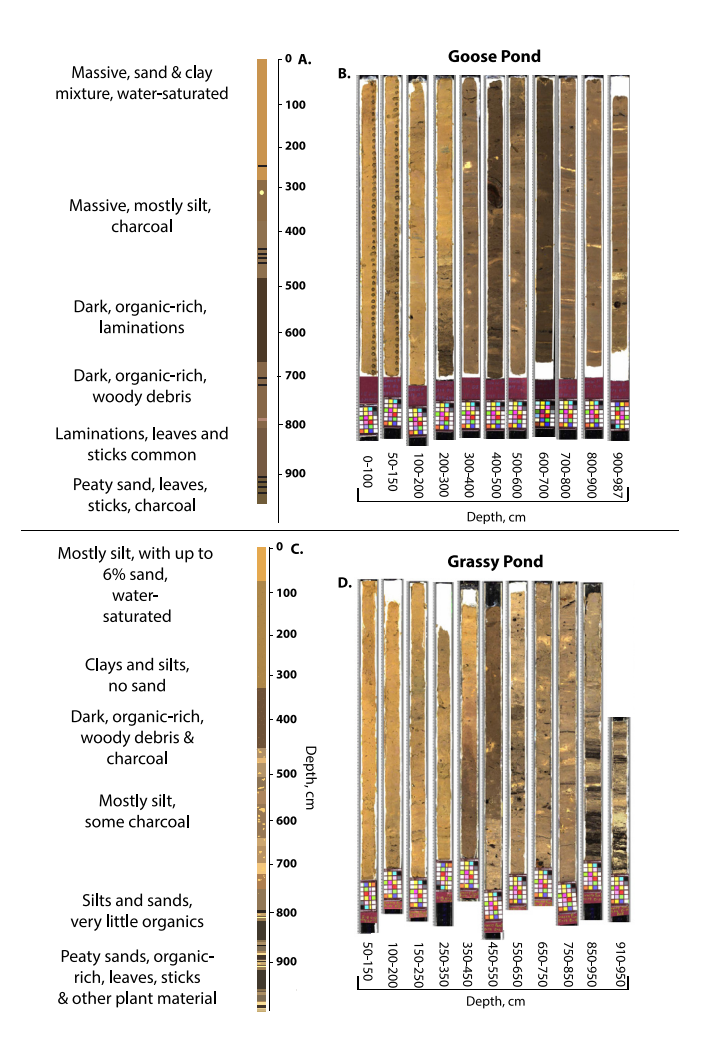


Fig. 3. A (C). Simplified lithological diagram of the Goose Pond (Grassy Pond) sediments. **B (D).**Core photos of the Goose Pond (Grassy Pond) sediment core.

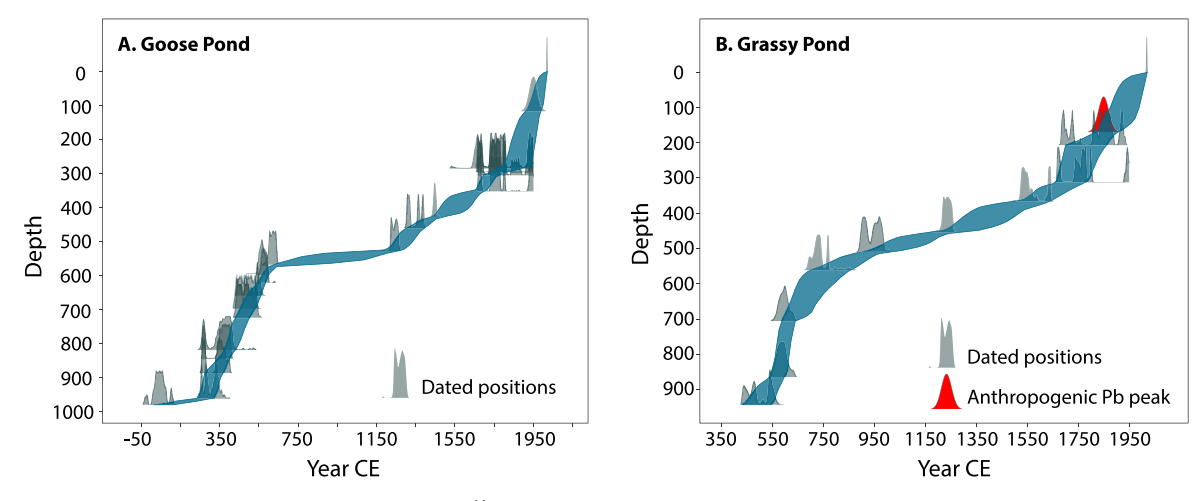


Fig. 4. Age models for **(A)** Goose and **(B)** Grassy ponds, constructed via ¹⁴C accelerator mass spectroscopy of terrestrially sourced macroscopic carbon (leaves, sticks, and charcoal). For Grassy Pond, the peak in modern Pb pollution was used as an additional geochronological anchor point at 1850 CE. Shaded blue area represents the 1-σ confidence intervals for each model.

Table 2Geochronology data used to constrain age-depth relationships at Goose and Grassy ponds.

Core	Depth	Fraction Modern	14C Age	+/-	Cal Yrs before present	Year CE
Goose Pond	1	N/A	-69	0		2019
Goose Pond	118	1.0555	0	20	0	1950
Goose Pond	282	0.9801	160	15	150	1800
Goose Pond	286	0.9748	205	40	155	1795
Goose Pond	297	0.9772	185	15	185	1765
Goose Pond	306	0.9817	150	15	220	1730
Goose Pond	353	0.9787	175	15	285	1665
Goose Pond	428	0.9468	440	15	500	1450
Goose Pond	461	0.9247	630	15	595	1355
Goose Pond	528	0.9033	815	15	715	1235
Goose Pond	568	0.8356	1445	15	1280	670
Goose Pond	594	0.8283	1515	15	1360	590
Goose Pond	621	0.8295	1500	15	1380	570
Goose Pond	661	0.8238	1555	15	1410	540
Goose Pond	698	0.8205	1590	15	1460	490
Goose Pond	725	0.8214	1580	15	1490	460
Goose Pond	819	0.8102	1690	35	1550	400
Goose Pond	844	0.8095	1700	15	1580	370
Goose Pond	886	0.8071	1720	15	1610	340
Goose Pond	961	0.8049	1745	15	1690	260
Goose Pond	979	0.7821	1975	15	1880	70
Grassy Pond	1	N/A	-69	0	-69	2019
Grassy Pond	170	N/A	100	20	90	1860
Grassy Pond	207.5	0.9843	125	15	140	1810
Grassy Pond	312.5	0.9777	180	15	270	1680
Grassy Pond	367	0.9631	300	15	400	1550
Grassy Pond	454	0.9039	810	15	705	1245
Grassy Pond	509.5	0.8718	1100	20	990	960
Grassy Pond	561.5	0.8565	1245	15	1160	790
Grassy Pond	706	0.833	1470	15	1320	630
Grassy Pond	864.5	0.8318	1480	20	1365	585
Grassy Pond	943	0.8256	1540	15	1410	540

600 CE. Sedimentation rates then decreased to 0.1 cm yr $^{-1}$ and remained comparatively low until 1220 CE. Between 1220 and 1260 CE, sedimentation rates increased to 1 cm yr $^{-1}$ and remained elevated until ca. 1820 CE. Sedimentation rates briefly declined between ca. 1820 and 1850 CE, after which sedimentation rates increased even further and reached 3 cm yr $^{-1}$ by 1940 CE. Between 1940 and 1980 CE, sedimentation rates decreased to 2.5 cm yr $^{-1}$ (Fig. 9 C.)

The Grassy Pond age model was developed using 9 AMS ¹⁴C-dated pieces of detrital terrestrial organics, the beginning of

anthropogenic Pb pollution at ~1850 CE (Fig. 5 A), and the modern sediment-water interface at 2019 CE (Fig. 4 B; Table 2). A $^{14}\mathrm{C}$ date from 26 cm above the basal sand unit indicated that the full sedimentary record of Grassy Pond spans approximately the last 1500 years.

Mean sedimentation rates at Grassy were high during the early section of the record, reaching a peak of 3 cm yr^{-1} at approximately 600 CE. Sedimentation rates began to decline after 700 CE and reached their lowest point in the record (0.2 cm yr⁻¹) by approximately 1000 CE. Between 1000 and 1230 CE, sedimentation rates

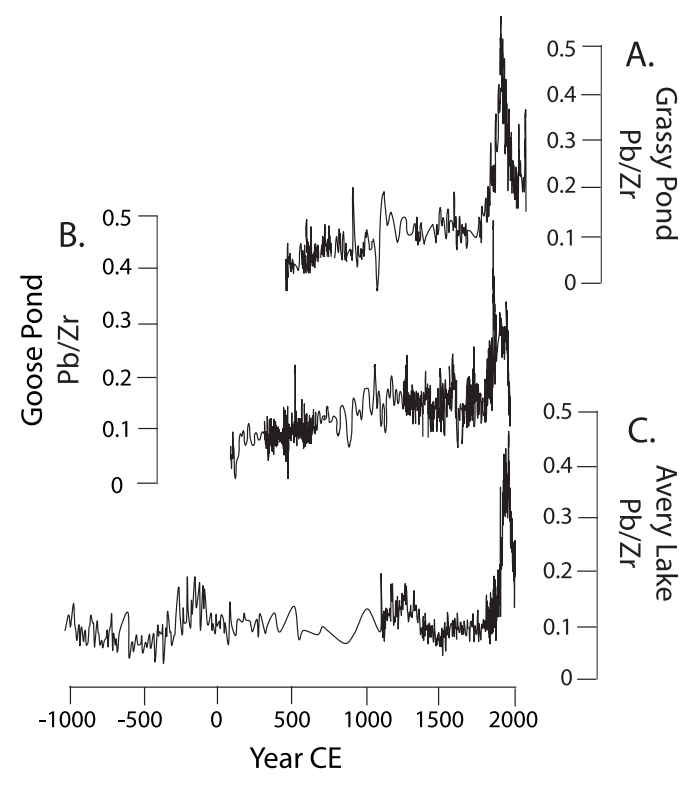


Fig. 5. X-Ray fluorescence data from Grassy Pond (**A**), Goose Pond (**B**), and Avery Lake (C; Bird et al., 2019). Zr-normalized Pb values were used as an indicator of excess Pb pollution. In particular, the large Pb/Zr peaks observed at all three lakes between 1800 and 1850 CE were interpreted as an indicator of Euro-American settlement and industrialization.

remained low. After 1230 CE, sedimentation rates increased to 0.25 cm yr $^{-1}$. Between 1230 and 1750 CE, sedimentation rates continued to increase - to 0.3 cm yr $^{-1}$ ca. 1540 CE - and 0.5 cm yr $^{-1}$ ca. 1750. Ca. 1850 CE, sedimentation rates increased again and reached 1 cm yr $^{-1}$. Sedimentation rates at Grassy Pond subsequently remained high until the present (Fig. 9 B).

4.3. Sediment grain size

The distribution of grain sizes at Goose and Grassy ponds were characterized by a general predominance of silt throughout each record, punctuated by intervals of sand-sized grains. At Goose Pond, high sand abundances were present during the time interval between ca. 300 and 650 CE. During this time, %sand ranged from 0 to 60%, with an average of 16%. This interval coincided with the period of early high sedimentation rates at Goose Pond. Between 650 and 1500 CE, sand decreased and silt-sized particles dominated. After ca. 1500 CE, silt decreased while sand and clav increased. Sand remained generally elevated throughout the rest of the record and reached its highest values between 1800 and 1850 CE (with an average of 37% sand during that interval). Between 1850 CE and the present, %sand declined, but remained relatively high compared to the rest of the record (Fig. 6 D). Proxies of grain size - magnetic susceptibility and Si/Al ratios - generally tracked grain size measurements at Goose Pond. Si/Al values at Goose Pond were high between 300 and 620 CE, lowest between 620 and 1250 CE, variable but generally elevated between 1250 and 1830 CE, and high between 1830 CE and the present (Fig. 6 B). Similarly, magnetic susceptibility was high between 300 and 600 CE (ranging

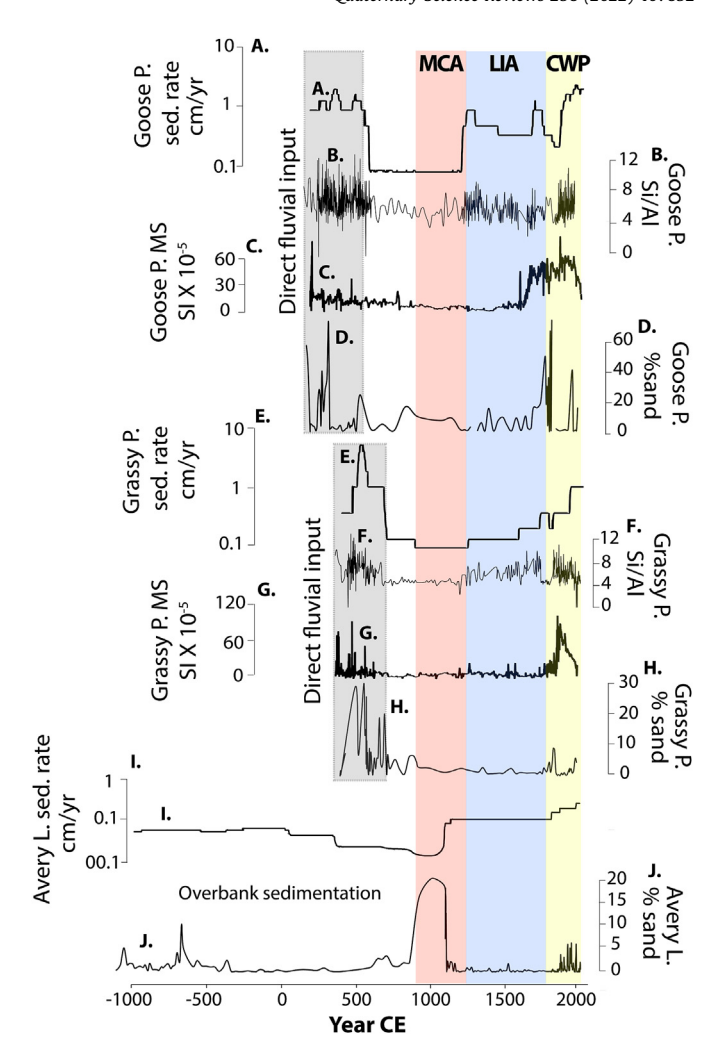


Fig. 6. The sand fraction of the **(A)** Goose Pond, **(B)** Grassy Pond, and **(C)** Avery Lake sediment cores, compared with the sedimentation rates at each site **(D-F,** respectively). At Goose and Grassy ponds, the period of high sedimentation rates during the early section of each record corresponded with large sand fractions — consistent with high energy, direct fluvial input during those times. At Avery Lake, the oldest section of lacustrine sediments did not show the same high levels of sand, suggesting that lower energy, overbank sedimentation occurred during flood events at Avery Lake even immediately after its formation.

from 9 to 79 SI x 10^{-5}), low between 600 and 1430 CE (ranging from 1 to 12 SI x 10^{-5}), high between 1430 and 1850 CE (3–60 SI x 10^{-5}), and highest between 1850 and the present (20–84 SI x 10^{-5}) (Fig. 6 C).

At Grassy Pond, relatively high sand abundances characterized the period spanning ca. 500 to 750 CE. During this period, %sand ranged from 0 to 31%, with an average of 10%. Similar to Goose Pond, the timing of the high sand abundances coincided with the period of early high sedimentation at Grassy Pond. Between 750 and 1540 CE, %sand decreased and the Grassy Pond core became dominated by silt-sized particles, with silt comprising between 60 and 80% of the sediments during this span. Between 1540 and 1800 CE, the Grassy Pond sediments were generally silt-dominated, punctuated by sandy intervals at 1570 and 1670 CE. After 1830 CE, %sand increased and remained relatively high until the present; however, silt remained the dominant grain size (Fig. 6 H). As with Goose Pond, the Grassy Pond Si/Al ratios and magnetic susceptibility were in-phase with grain size measurements (Fig. 6 F & G).

4.4. Isotopic composition of total nitrogen

Between ca. 300 and 600 CE, δ^{15} N values at Goose Pond were moderately high, with an average of 4.05‰. δ^{15} N values subsequently gradually decreased until reaching their lowest point (2.33‰) ca. 1520 CE. δ^{15} N remained low until ca. 1670 CE, at which point δ^{15} N increased abruptly and reached their highest values (6.82‰) ca. 1880. δ^{15} N decreased slightly after 1880 CE, but remained comparatively high until the present.

At Grassy Pond, $\delta^{15}N$ ranged between 1.78 and 6.79% (Fig. 7). Between ca. 430–940 CE, $\delta^{15}N$ averaged 3.71%. $\delta^{15}N$ values were low between ca. 1100 CE and ca. 1600 CE, including the lowest $\delta^{15}N$ value of the record (1.78%) at ca. 1300 CE. After ca. 1600 CE, $\delta^{15}N$ increased to 5.64% and remained high (averaging 5.46% and reaching as high as 6.07%) until ca. 1800. Between ca. 1800 and 1850, $\delta^{15}N$ values decreased slightly to 5.55%, then rose again to their highest point (6.79%) in 1910 CE. Between 1910 CE and the present, $\delta^{15}N$ values decreased slightly, but remained as high or higher than any other point in the Grassy Pond record (Fig. 7).

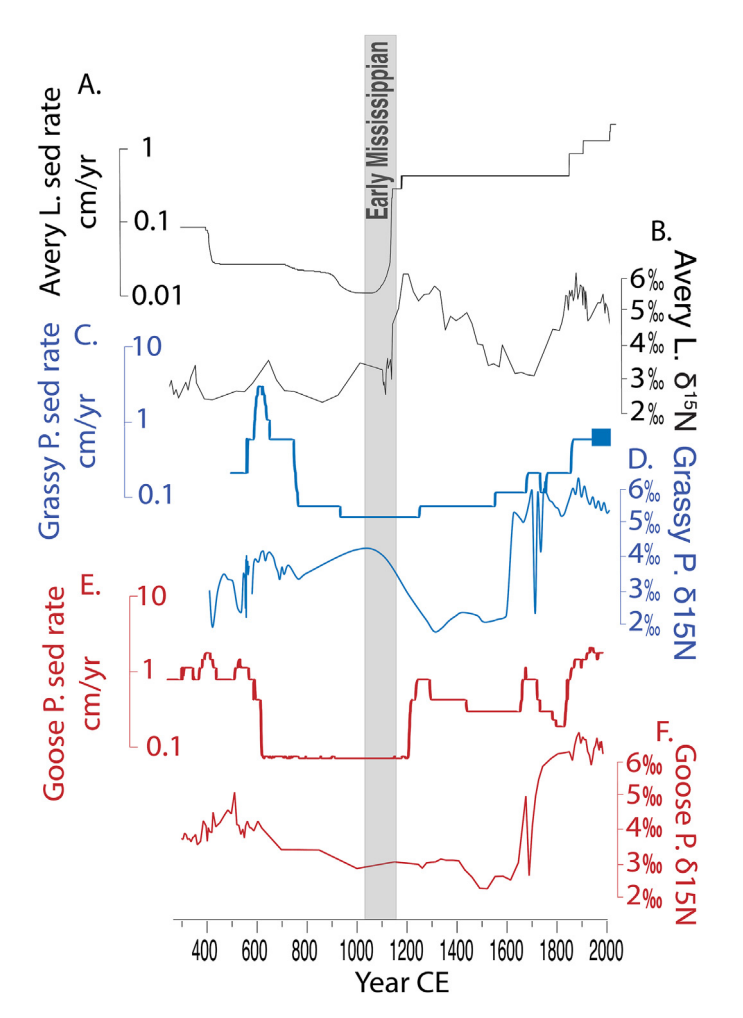


Fig. 7. Sedimentation rates and $\delta^{15}N$ from Avery Lake (**A** and **B**; Bird et al., 2019), Grassy Pond (**C** and **D**), and Goose Pond (**E** and **F**). At Avery Lake, an abrupt and substantial increase in $\delta^{15}N$ coincided with the increase in sedimentation that was observed to have occurred ca. 1100 CE, suggesting that Mississippian occupation and land-use at the Avery site may have been responsible for increased sedimentation during this time.

5. Discussion

5.1. Floodplain lake sedimentation rates on the lower Ohio River

Records of fluvial processes, especially flooding, are difficult to produce without stream gage data, and long paleo-records of flood frequencies are rare. Since sediment accumulation in floodplain lakes is driven largely by flooding of the adjacent river, these sedimentary records provide an important archive of past flood events and can be used to reconstruct the recurrence of flooding over millennial-scale timescales (Munoz et al., 2014; Oliva et al., 2016; Toonen et al., 2016; Bird et al., 2019). In addition, stream gage data mostly record fluvial dynamics that are occurring in an anthropogenically-altered landscape, so flood reconstructions based on sedimentation rates on floodplains and in floodplain lakes are especially useful for understanding preindustrial linkages between natural climatic variability and fluvial responses.

Late Holocene sedimentation rates at Goose and Grassy ponds show good general agreement, but with important differences during the early portion of each record. While both lakes experienced exceptionally high sedimentation rates for approximately 200-250 years after their formation, the timing of these high sedimentation rate periods was different between the sites. As the older of the two swale lakes, Goose Pond experienced high sedimentation rates from 300 to 550 CE with subsequently low sedimentation rates thereafter until 1250 CE. Grassy pond similarly experienced high sedimentation rates for approximately 200 years after its formation (between 500 and 750 CE), but this period occurred when sedimentation rates at Goose Pond had already decreased. The difference in the timing of these high sedimentation rate periods could suggest that each site experienced different flood inundation histories; however, both sites are located within 6 km of each other on the same reach of the Ohio River and are situated at similar elevations on their respective floodplains. It is therefore improbable that flooding histories at these sites would have substantially differed. Instead, it is more likely that geomorphic processes related to swale lake formation were responsible for the accumulation rate differences.

One possibility is that the periods of high sedimentation rates immediately following the formation of the respective swale lakes reflects direct fluvial input of sediment-laden waters from the main channel of the Ohio River. This is likely to have occurred during the first few hundred years after each lake formed given the proximity and orientation of the Ohio River to the swale lakes immediately after their formation. Meander scars visible in high resolution LiDAR data between the Ohio River and the floodplain lakes show that the Ohio River was initially nearly parallel to the newly formed swales, which would have allowed it to transport large amounts of sediment directly into the swales, as has been observed in other fluvial systems (Fig. 1) (Constantine et al., 2010). In this model, Goose and Grassy ponds would have been directly in the path of high-energy discharge during Ohio River flood events for 200 (Grassy Pond) to 250 (Goose Pond) years following each lake's respective formation. During these events, the Ohio River would have been in extremely close proximity and in a similar orientation to the newly formed swale lakes, thereby directing high-energy, sediment-laden discharge through these systems. As the Ohio River continued to migrate and build out the local floodplains, the distance and angle between the main Ohio River channel and Goose and Grassy ponds changed such that the Ohio River was both further away and directing high energy flow away from the swale lakes during overbank discharge events. This would have ultimately directed the highest energy, most sediment-laden discharge away from Goose and Grassy ponds during flood events. Instead, the swale lakes would have been inundated with lower energy

overbank flows during floods that lack the competence to transport the coarser grained sediments characteristic of the higher energy main fluvial channel. Since Goose Pond is approximately 200 years older than Grassy Pond, the Ohio River would have begun and finished transmitting fluvial sediments directly into the Goose Pond swale during flood events earlier than Grassy Pond, which is consistent with the difference in timing of the early high-sedimentation rate periods at both lakes (Fig. 9 B & C).

This model of early swale lake formation and evolution is in agreement with grain size records from Goose and Grassy ponds (Fig. 6). For both lakes, sand abundances (averaging 15% at Goose Pond and 10% Grassy Pond) were high during the first 200-250 years of each record when sedimentation rates were highest. This is consistent with high energy deposition as a result of direct fluvial input immediately after the lakes formed, when the Ohio River was both immediately adjacent and oriented in line with the newly formed swale lakes. Sedimentation rates and %sand both decreased at Goose and Grassy ponds after their respective early high sedimentation rate phases. Notably, when sedimentation rates at Goose and Grassy ponds increased again ca. 1250 CE, %sand at both sites remained lower than the periods immediately after the formation of each lake. This indicates that sand abundances during the first 200-250 years of each record were not linked to sediment accumulation rates alone and suggests that the combination of high sedimentation rates and high sand abundances early in the Goose and Grassy pond sediment archives were a result of direct, higherenergy, fluvial input from the adjacent and nearly parallel Ohio River for approximately 200–250 years after the swale lakes formed. Once enough floodplain had been constructed between the swale lakes and the Ohio River and the angle of the Ohio River relative to the swale lakes had changed, sedimentation rates were controlled by lower-energy overbank deposition and both lakes became silt-dominated systems, even during periods when flooding was frequent (Fig. 8).

In contrast with Goose and Grassy ponds, the Avery Lake record did not experience a period of high sedimentation rates immediately following the lake's formation at 1150 BCE. The bottom 7 cm of the Avery Lake sediment core was characterized by sand and gravel, which were interpreted to represent bedload sediments of the active Ohio River, deposited prior to the formation of Avery Lake (Bird et al., 2019). Above this section, sedimentation rates at Avery Lake were comparatively consistent for ca. 1500 years after the lake's formation and grain sizes were consistently dominated by silt and clay with little to no sand. This difference in the early portion of the Avery Lake record relative to Goose and Grassy ponds is consistent with the different nature of flooding that occurs at Avery Lake as compared to the other two sites as a result of different point bar morphometries (Alexander and Prior, 1971; see also section 2.3).

Taken together, the combination of the Goose Pond, Grassy Pond, and Avery Lake sedimentation and grain size records suggests that fluvial geomorphic processes resulted in high sedimentation rates at Goose and Grassy ponds immediately after their respective formations and that overbank deposition became dominant once the floodplain had built out enough that the orientation of the Ohio River no longer directed high-energy, sediment-laden discharge directly into the newly formed swales. Once overbank sedimentation was established at each site, sedimentation rates show good agreement, suggesting they reflect changes in the frequency of overbank deposition events driven by Ohio River flooding.

5.2. Late Holocene flooding on the lower Ohio River

Overbank sedimentation rates on the lower Ohio River prior to

the onset of Euro-American deforestation and industrialization in the Midwest during the 1800s and 1900s (Greeley, 1925; Page and Walker, 1991) are divided into two distinct phases. The first phase was characterized by low sedimentation rates between 400 and 1100 CE at Avery Lake, 600 to 1230 CE at Goose Pond, and 750 to 1230 CE at Grassy Pond. This period includes the MCA, during which time sedimentation rates at all three sites reached their lowest values (Fig. 9A-C). Concomitant with the reduced sedimentation rates, sedimentological and geochemical proxies (i.e., Si/ Al ratios, and magnetic susceptibility) from Goose and Grassy ponds indicate reduced local erosion and/or low depositional energy (Fig. 6), supporting the hypothesis that overbank sediment delivery to these sites was low due to a prolonged reduction in regional flood frequencies between 400 and 1200 CE. Sedimentation rates at Avery Lake increased abruptly near the end of the MCA between 1100 and 1150 CE and remained moderately high for the next 800 years throughout the LIA (Bird et al., 2019), while sedimentation rates at Goose and Grassy ponds did not increase until the end of the MCA at ca. 1250 CE.

The earlier increase in sedimentation rates at Avery Lake at ca. 1100 CE relative to Goose and Grassy ponds could suggest an increase in flood frequency on the Avery Lake point bar that did not impact the Ohio River by Goose or Grassy ponds. However, Avery Lake is situated at a higher elevation relative to the Ohio River than Goose and Grassy ponds. Therefore, a similar increase in sedimentation rates at all three sites would be expected if increased sedimentation rates at Avery Lake between 1100 and 1150 CE were due to an increase in floods with discharges capable of inundating the site. The difference between the Avery Lake record and the Goose and Grassy pond records therefore suggests that Avery Lake's sedimentation rate increase at ca. 1100 CE may have been related to a different, perhaps local, mechanism.

The sedimentation rate increase at Avery Lake at ca. 1100 CE notably occurred during the establishment of the Mississippian settlement at Kincaid Mounds. Between 1100 and 1150 CE, extensive maize agriculture was established (Bird et al., 2019; Commerford et al., 2022) and the monumental earth works were constructed (Muller, 2016). At the same time, $\delta^{15}N$ values and Ambrosia (ragweed) pollen - an indicator of deforestation increased markedly in the Avery Lake sediments, indicating that the floodplain surrounding Avery Lake supported a dense human population that impacted the landscape in ways that were comparable to the industrial era (Bird et al., 2019; Commerford et al., 2022). Although a small Native American settlement existed near Goose Pond during Middle Woodland era (between 200 and 500 CE) (Doperalski, 2017), $\delta^{15}N$ data from both Goose and Grassy ponds show no evidence for significant pre-European human impact and both sites lack any adjacent monumental earth works. We therefore suggest that the early increase in sedimentation rates at Avery Lake relative to Goose and Grassy ponds during the transition from the MCA to the LIA reflects anthropogenic activity at Kincaid Mounds, and that the continued low sedimentation rates at Goose and Grassy ponds reflects infrequent overbank discharges on the Ohio River during the late MCA in response to reduced snowpacks and infrequent flooding in the Ohio River Valley.

Circa 1230 CE, overbank sedimentation at Goose and Grassy ponds began to increase rapidly, achieving sustained high rates by 1250 CE, which corresponds with transition from the MCA to the LIA in the Midwest (Bird et al., 2017). Due to the lack of significant human landscape disturbances at these sites, the good temporal correspondence of increasing sedimentation rates at Goose and Grassy ponds likely provides a more robust estimate for the Ohio River's response to regional climatic changes that occurred during the LIA. Specifically, the increase in sedimentation rates between 1230 and 1250 suggests that flooding on the Ohio River increased

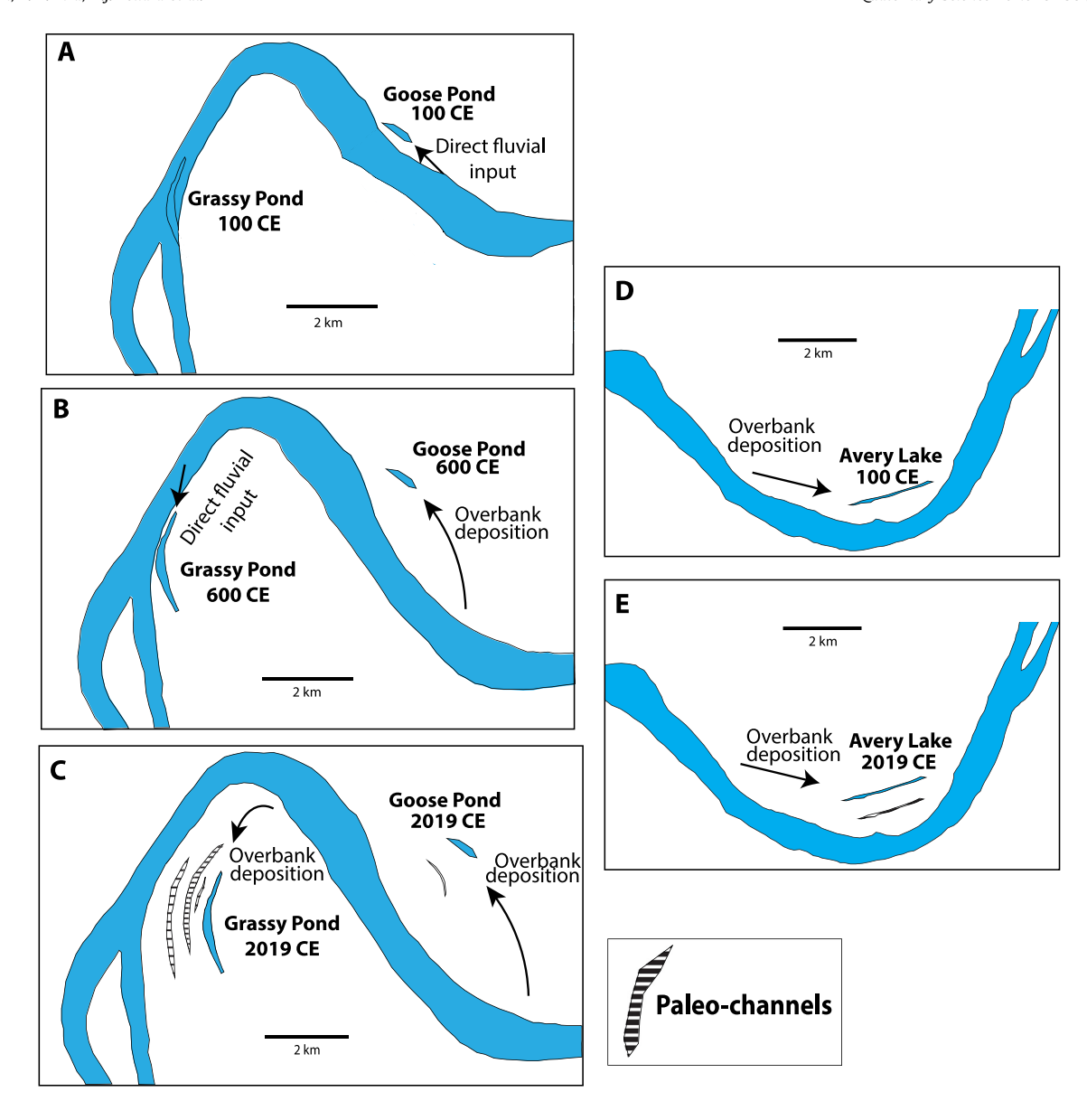


Fig. 8. Conceptual schematic of the different flooding styles that impacted Avery Lake and Goose and Grassy ponds. (A) Ca. 100 CE, soon after the formation of Goose Pond and before the formation of Grassy Pond, Goose Pond received primarily high energy floodwaters directly from the Ohio River during flood events. (B) By ca. 500 CE, migration of the Ohio River resulted in low energy overbank sedimentation at Goose Pond, while high energy deposits impacted the newly formed Grassy Pond. (C) As the meandering Ohio River continued to build the floodplains around Goose and Grassy ponds, the distance and angle between the main river channel and the floodplains lakes increased such that low energy, overbank sedimentation eventually dominated at both sites. (D, E) At Avery Lake, however, overbank sedimentation dominated throughout the record, due to the morphometry of the Black Bottom floodplain.

during this time in response to increases in regional snowpack during the LIA.

From 1250 CE until the onset of industrialization at ca. 1800 CE, sedimentation rates were consistently high at all three floodplain lakes. Clastic input and magnetic susceptibility also increased during this time, indicating that erosion and runoff were enhanced and further supporting that flooding became more frequent during this period. Importantly, by the 1400s CE, *Ambrosia* and arboreal pollen in the Avery Lake core returned to pre-Mississippian levels, but sedimentation rates remained high, indicating that sediment delivery to Avery Lake remained high even after the local watershed became reforested and the impacts of Mississippian land use were diminished (Bird et al., 2019). These characteristics suggest that, while the early sedimentation rate increase (i.e., from 1100 to 1150 CE) at Avery Lake may have been due to local Mississippian

landscape disturbance, sedimentation rates remained high through the LIA due to an increase in overbank alluvial sedimentation during Ohio River flood events, like Goose and Grassy ponds.

Aside from the anthropogenic influences at Avery Lake during the Early Mississippian Period (1050–1150 CE), the overbank sedimentation rates at Avery Lake, Goose Pond, and Grassy Pond were generally in-phase over the past ca. 1300 years. These results indicate that flood frequency on the lower Ohio River was regionally coherent during the late Holocene and suggests that flooding of the Ohio River at large was responsive to a common climatic driver (Fig. 9). In addition to the floodplain records from the Ohio River presented here, previously published flood recurrence records from the upper Mississippi Valley further suggest reduced flood frequencies on large rivers in the Midwestern US during the MCA and increased flooding during the LIA (Munoz et al., 2015; Lombardi

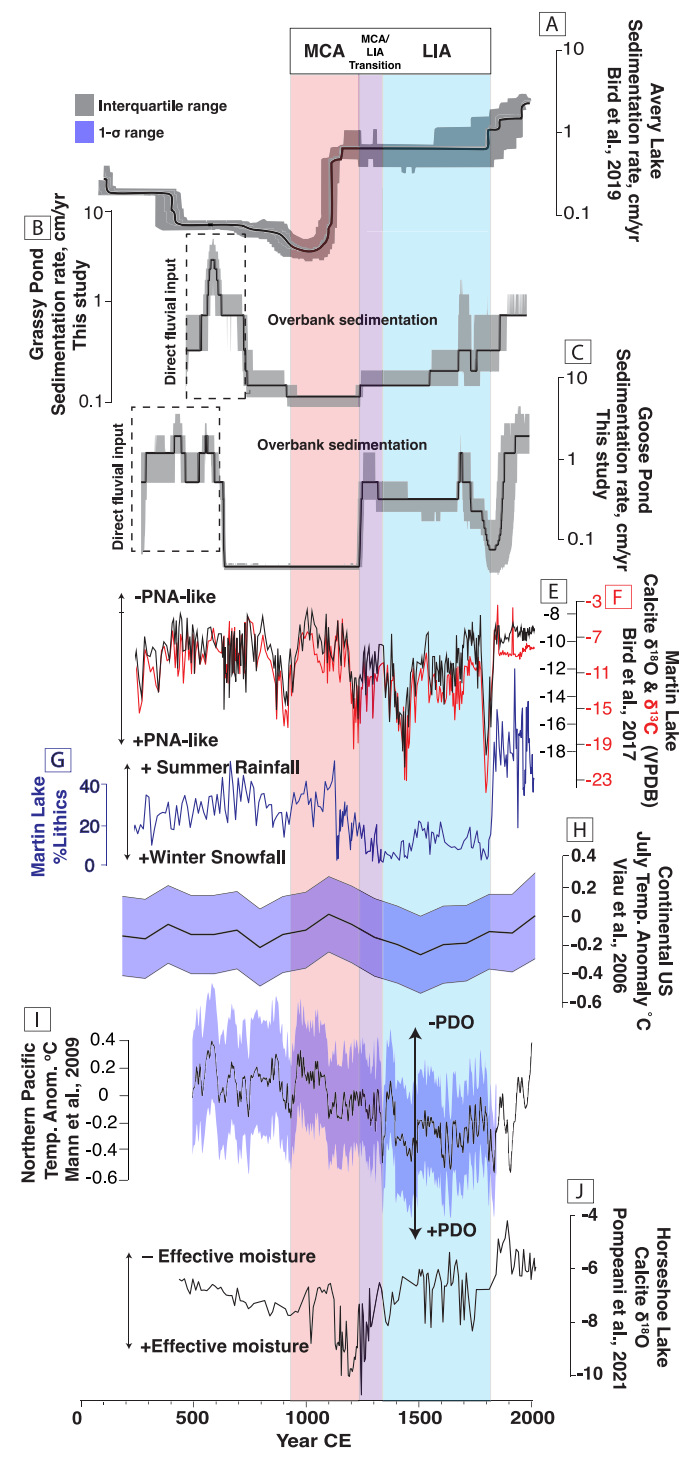


Fig. 9. Late Holocene proxies for paleoclimatic conditions and flood recurrence in the midcontinental US. Median sedimentation rates at **A.** Avery Lake (Bird et al., 2019), **B.** Grassy Pond, and **C.** Goose Pond are represented by bold black lines, with 1- σ confidence intervals represented by the shaded gray areas. These results are compared with E. Martin Lake $\delta^{18}O$ and **F.** $\delta^{13}C$, which were used as proxies for precipitation source and warm-season length (thermal stratification), respectively, and Martin Lake % lithic abundances, **G.**, which were interpreted as a proxy for watershed erosion and transport, driven primarily by convective rainstorms (Bird et al., 2017). Continental average surface temperatures during the late Holocene, **H.**, were determined by fossil pollen assemblages (Viau et al., 2006), while late Holocene northern Pacific SSTs, **I.**, were constrained using a multi-proxy dataset (Mann et al., 2009). Effective moisture in the midcontinental United States, **J.**, was determined by the relative enrichment or depletion of calcite $\delta^{18}O$ from Horseshoe Lake, IL (Pompeani et al., 2021).

et al., 2021).

5.3. Ohio River flooding and regional climate

Coherent sedimentation rates at the three floodplain lakes presented here indicate similar flood histories on the lower Ohio River. This is consistent with modern patterns of flooding in the Ohio River Valley, across which flooding occurs at approximately the same time during the spring months (Fig. 2). Given the similar timing of flooding across the Ohio River Valley today and that flooding on large fluvial systems like the Ohio River is primarily driven by watershed-scale snowmelt (Knox, 1988, 2000), we interpret the sedimentation rate records presented here to largely reflect variability in flooding of the Ohio River at large due to variations in snowpack. Previous work at Avery Lake suggested that the occurrence of flooding on the lower Ohio River was linked to mean state changes in synoptic-scale atmospheric circulation that either enhanced or diminished winter snowpack, which correspondingly increased or decreased flood frequency (Bird et al., 2019). Together, the Avery Lake and Goose and Grassy pond records provide a coherent and consistent picture of lower Ohio River flooding that, when compared with Midwest paleoclimate records, allows the previously suggested Ohio River climate-flood relationships to be tested. These new records support the contention that Ohio River flood frequencies were low prior to and during the MCA (from ca. 400 to the early 1200s CE), when paleoclimate data indicate diminished winter-like and extended wet warm-season atmospheric conditions with ample rainfall sourced predominantly from the Gulf of Mexico (Fig. 9, E. H. & I: Bird et al., 2017). Infrequent flooding on the Ohio River under wet warm-season conditions is consistent with the response of high-order streams with large watersheds to rainstorms versus snowpack melt (Knox, 2000). Specifically, prior to modern land use practices, large streams like the Ohio River (ca. 420,000 km² watershed; Schilling et al., 2015) were unlikely to flood as a result of individual warmseason rainstorm events because their watersheds are simply too large for any one precipitation event to completely envelop it. Therefore, while convective storms likely had the potential to cause flooding at the local scale along the smaller tributaries of the Ohio River (Lavers and Villarini, 2013; Bird et al., 2017; Wright, 2022), they were unlikely to have produced runoff magnitudes sufficient to drive large-scale flooding along the lower Ohio River (Knox, 2000; Bird et al., 2019). Additionally, the warm-season-like conditions before 1250 CE (Fig. 9 F) likely increased the duration and extent of evapotranspiration while reducing the amount of time that the landscape was frozen, thereby increasing infiltration and reducing runoff (e.g., Bosch and Hewlett, 1982).

Between 1220 and 1250 CE, increased sediment delivery to Goose and Grassy ponds coincided with a regional shift toward winter-like conditions across the midcontinental United States during the transition to the LIA (Bird et al., 2017). Increased Ohio River flooding during the LIA occurred as near-surface air temperatures in the midcontinental United States cooled (Viau et al., 2006) (Fig. 9 H), meridional mean-state atmospheric circulation increased the incursion of airmasses from the northern Pacific, and precipitation seasonality shifted to winter-dominated (Bird et al., 2017) (Fig. 9E-G). Resembling a +PNA-like mean state (Bird et al., 2017), it is likely that greater amounts of snow accumulated across the eastern United States each year due to the prolonged cold season and predominance of northerly-sourced winter precipitation (e.g., Serreze et al., 1998). During this time, increased snowpack melt in the Ohio River Valley during the spring would have released multiple precipitation events worth of water over a short period of time (likely weeks), which would have been integrated into the Ohio River and resulted in the regular occurrence of high discharge events. Additionally, cooler temperatures during the LIA may have contributed to enhanced runoff as a result of more deeply frozen ground, reduced vegetation, and diminished evapotranspiration. We hypothesize that these conditions were enough to increase Ohio River flooding even though overall precipitation during this time was diminished (BoothNotaro et al., 2006; Pompeani et al., 2021, Fig. 9 J).

In summary, the paleoclimate-flood relationships detailed above show good correspondence with reconstructions of oceanatmosphere teleconnections that are known to affect Midwestern stream flow through their influence on precipitation today. During the late Holocene, mean-state atmospheric circulation across the United States fluctuated in ways that resembled variability associated with the PNA (Bird et al., 2017). These changes were generally in-phase with, and likely driven by, sea surface temperature (SST) variability in the northern Pacific Ocean (Fig. 9 J; Yu and Zwiers, 2007; Mann et al., 2009). Specifically, SSTs in the northern Pacific were anomalously warm during the MCA (i.e., -PDO conditions) (Mann et al., 2009), which has been shown to create a midtropospheric trough in the western US and a sustained ridge over the northeastern US today (Yu et al., 2007). This in turn likely promoted mean-state conditions that resembled the -PNA mode (i.e., a more zonal jet stream that enhanced clockwise atmospheric circulation over the eastern half of the US), which would have increased Ohio River Valley summer rainfall sourced from the Gulf of Mexico, decreased snowpack volume across the Ohio River Valley, and ultimately decreased the frequency of Ohio River flooding. During the LIA, northern Pacific SSTs were anomalously cool (i.e., +PDO conditions), which promoted + PNA-like meanstate atmospheric conditions over the United States. These conditions were characterized by a broad mid-tropospheric trough across most of the eastern United States during the winter months (Coleman and Rogers, 2003). Consequently, summer precipitation (rainfall) was likely diminished, while winter precipitation (snowfall/snowpack) was likely increased across the Ohio River Valley (Serreze et al., 1998), resulting in an increase in flood frequency on the Ohio River during the LIA.

5.4. Ohio River flood recurrence post 1800 CE

After ca. 1800 CE, Midwestern isotope records (Fig. 9 E, F, & I) indicate a return to southerly atmospheric circulation, an increase in warm-season precipitation, and a reduction in cold-season precipitation (i.e., snowpack). Overbank sedimentation rates in the Ohio River floodplain lakes, however, increased to their highest values instead of decreasing as they did between 500 and 1250 CE when atmospheric conditions similar to today prevailed. It is possible that the observed modern increase in sediment accumulation, and thus, flood recurrence, recorded in the floodplain lakes is due solely to modern climate dynamics. Extreme (99th percentile) precipitation events have increased by more than 40% since the mid 1900's (Easterling et al., 2017). These precipitation events are also ocurring earlier in the spring and later in the fall than any other time in instrumental history, partially as a result of lengthening summer-like conditions driven by modern climate change (Pryor et al., 2014). However, the modern increase in flooding on the Ohio River occurred prior to the observed increase in precipitation and individual precipitation events are generally not capable of producing watershed-scale flood events across large basins like the Ohio River Valley (Knox, 2000; Bird et al., 2019). It is therefore likely that additional factors are responsible for the increase in flood frequency observed after 1800 CE.

Superimposed on the transition to conditions dominated by warm season precipitation during the current warm period (CWP; last ca. 150 years) is the occurrence of widespread deforestation for

row crop agriculture and urbanization across much of the eastern United States that began in the early 1800s CE (Greeley, 1925). These land use changes intensified after 1850 CE such that by 1920 nearly 100% of old-growth forest had been removed from the Ohio River watershed (Greeley, 1925). As result, interception and evapotranspiration of precipitation has likely been significantly reduced, allowing a greater percentage of precipitation to directly enter the Ohio River and its tributaries, and thereby increasing the responsiveness of the Ohio River to discrete warm-season rainstorms. In addition to deforestation, wetland removal and tile drainage for agriculture that began in the mid-1800s has further impacted Midwestern hydrology (Beauchamp, 1987) by reducing the flood-buffering capability of the landscape and increasing the rate and amount of runoff that enters the Ohio River and its tributaries (Smith et al., 2015).

We therefore attribute the observed recent decoupling from preindustrial flood-climate relationships to increased runoff caused by a combination of modern climate change and the large-scale Euro-American land clearance that occurred across the Ohio River Valley during the CWP. The increase in modern precipitation, combined with deforestation, has likely created a new hydrologic regime across the Ohio River Valley in which flood events are more common than any other time during the past ca. 3000 years and are likely to further increase over the next several decades in response to predicted precipitation increases by mid-century (Easterling et al., 2017).

Since the observed increase in modern flooding appears to be due, at least in part, to rapid runoff, methods that slow the return of precipitation to the Ohio River and its tributaries have the potential to mitigate modern flood hazards (e.g., van Noordwijk et al., 2017). In the Midwest, one way of achieving this is through the preservation of existing, and construction of new, riparian wetlands. Riparian wetlands adjacent to fluvial systems intercept runoff before it reaches the river channel, reducing the rate and volume of precipitation that enters streams after precipitation events (Schultz et al., 2004). New wetlands, created to act as diversions from the streams themselves during high discharge events, can also be used to remove excess water from tributaries during high discharge events, ultimately reducing the amount of dischage that enters higher-order streams in the watershed and reducing the risk for catastrophic flooding (e.g., Mitsch and Day Jr., 2006). Given that precipitation – and particularly extreme precipitation events – are projected to increase over the next few decades, the preservation and creation of riparian wetland buffer zones is an important flood mitigation strategy that should be implemented across the Ohio River Valley.

6. Conclusions

Late Holocene meandering of the Ohio River created numerous point bars and floodplains across the lower Ohio River Valley. These landscapes retain geomorphic evidence of past Ohio River mobility, including the terraces of paleo-floodplains and depressions left behind by past fluvial channels. Of the latter, paleochannel lakes are shown here to be valuable recorders of past fluvial dynamics, such as floodplain development and flood recurrence.

Sedimentation rates from two swale lakes located in Kentucky and Indiana were used as proxies for Ohio River flood recurrence through time and synthesized with the only other currently published sedimentation-based Ohio River flood record. Good general agreement between the three records over the past 1900 years indicates that late Holocene flooding on the lower Ohio River was regionally coherent. Furthermore, the synoptic-scale atmospheric conditions associated with the PNA and PDO impact much of the eastern United States and influence the seasonality, amount, and

phase of precipitation across the entirety of the Ohio River Valley (Coleman and Rogers, 2003; Goodrich and Walker, 2011; Mills and Walsh, 2013). As a result, the timing and magnitude of basin-scale changes in discharge across the Ohio River Valley are similar on seasonal and annual time scales (Fig. 2 & Table 1). The flood records presented here from the lower Ohio River are therefore likely regional-scale recorders of the impact of these synoptic-scale climatic processes and likely reflect flood recurrence along the entire Ohio River, although similar upstream paleo-flood records would be necessary to confirm this hypothesis.

The sedimentation rate records presented here indicate that Ohio River flooding was least frequent between ca. 400 and 1200 CE. When combined with regional paleoclimate data, these records suggest that persistently warm conditions and mean-state atmospheric circulation that resembled the -PNA mode prior to and during the MCA decreased winter precipitation and snowpack, resulting in a regional reduction of flood events. During the transition to the LIA, atmospheric circulation over the Ohio River Valley switched to mean-state conditions resembling the +PNA, with meridional atmospheric flow and an increase in winter precipitation/snowpack, which consequently increased the frequency of Ohio River flood events. The predominance of winter precipitation and frequent flooding continued through the LIA until the onset of the CWP, ca. 150 years ago. Circa 1800 CE, the seasonality of precipitation returned to summer-dominated, and atmospheric circulation over the Ohio River Valley returned to clockwise, zonal flow – conditions associated with reduced flood frequency in the paleo-record. However, floodplain sedimentation rates indicate that flooding increased even further and became more frequent than any other time of the past 1600 years. This decoupling from the relationships observed in the paleo-record suggest that modern anthropogenic land use and climate change has altered the Midwestern hydrologic cycle such that the Ohio River is now susceptible to flood events driven by both snowmelt and discrete warmseason precipitation events.

Funding sources

This work was supported by the National Science Foundation (grant # EAR-1903628) and the Nature Conservancy (grant # 2041–002).

Author contribution

Derek Gibson: Writing — original draft; Writing — review & editing; Investigation; Formal analysis; Visualization; Data curation, **Broxton Bird**: Writing — review & editing; Conceptualization; Funding acquisition; Methodology; Supervision, **Harvie pollard**: Writing — original draft; Formal analysis; Investigation; Visualization; Data curation, **Cameron Nealy**: Writing — review & editing; Formal analysis; Investigation; Data curation, **Robert Barr**: Writing — review & editing; Methodology, **Jaime Escobar**: Formal analysis; Investigation; Data curation.

Declaration of competing interest

The authors declare that they have no known competing financial interests or personal relationships that could have appeared to influence the work reported in this paper.

Data availability

All original data is archived on the NOAA Paleoclimate database (https://www.ncei.noaa.gov/access/paleo-search/study/37022) and on Mendalay (Gibson, Derek (2022), "Grassy Pond composite

data book", Mendeley Data, V3, doi: 10.17632/fh7gf2pvy8.3Gibson, Derek (2022), "Goose Pond composite data book", Mendeley Data, V3, doi: 10.17632/rfhh7twxc6.3)

References

- Abbott, M., Stafford, T., 1996. Radiocarbon geochemistry of modern and ancient arctic lake systems, baffin island, Canada. Quat. Res. 45 (3), 300–311. https://doi.org/10.1006/qres.1996.0031.
- Alexander, C.S., Nunnally, N.R., 1972. Channel stability on the lower Ohio River. Ann. Assoc. Am. Geogr. 62, 411–417.
- Alexander, C.S., Prior, J.C., 1968. The origin and function of the Cache Valley, southern Illinois. In: Bergstrom, R.E. (Ed.), The Quaternary of Illinois. Illinois Geological Survey, Urbana, IL, pp. 19–26.
- Alexander, C.S., Prior, J.C., 1971. Holocene sedimentation rates in overbank deposits in the Black Bottom of the lower Ohio River, southern Illinois. Am. J. Sci. 270 (5), 361–372.
- Andresen, J., Hilberg, S., Kunkel, K., 2012. Historical climate and climate trends in the midwestern USA. In: Winkler, J., Andresen, J., Hatfield, J., Bidwell, D., Brown, D. (Eds.), U.S. National Climate Assessment Midwest Technical Input Report, Coordinators. Available from the Great Lakes Integrated Sciences and Assessments (GLISA) Center. http://glisa.msu.edu/docs/NCA/MTIT_Historical.
- Archambault, H.M., Bosart, L.F., Keyser, D., Aiyyer, A.R., 2008. Influence of large-scale flow regimes on cool-season precipitation in the northeastern United States. Mon. Weather Rev. 136 (8), 2945–2963.
- Asselman, N.E.M., Middelkoop, H., 1995. Floodplain sedimentation: quantities, patterns and processes. Earth Surf. Process. Landforms 20, 481–499. https://doi.org/10.1002/esp.3290200602.
- Beauchamp, K.H., 1987. A history of drainage and drainage methods. Farm drainage in the United States: history, Status, and prospects. In: Pavelis, G.A. (Ed.), Miscellaneous Publication Number 1455. Economic Research Service (DOA), Washington, D.C.
- Bird, B.W., Barr, R.C., Commerford, J., et al., 2019. Late-Holocene floodplain development, land-use, and hydroclimate—flood relationships on the lower Ohio River, US. Holocene 29 (12), 1856–1870. https://doi.org/10.1177/0959683619865598.
- Bird, B.W., Wilson, J., Gilhooly III, W., et al., 2017. Midcontinental Native American population dynamics and late Holocene hydroclimate extremes. Sci. Rep. 7, 41628. https://doi.org/10.1038/srep41628.
- Birk, K., Lupo, A.R., Guinan, P., Barbieri, C.E., 2010. The interannual variability of midwestern temperatures and precipitation as related to the ENSO and PDO. Atmósfera 23 (2), 95–128.
- Boës, X., Rydberg, J., Martinez-Cortizas, A., Bindler, R., Renberg, I., 2011. Evaluation of conservative lithogenic elements (Ti, Zr, Al, and Rb) to study anthropogenic element enrichments in lake sediments. J. Paleolimnol. 46, 75–87.
- Booth, R.K., Notaro, M., Jackson, S.T., Kutzbach, J.E., 2006. Widespread drought episodes in the western Great Lakes region during the past 2000 years: geographic extent and potential mechanisms. Earth Planet Sci. Lett. 242, 415–427. https://doi.org/10.1016/j.epsl.2005.12.028. Issues 3–4.
- Bosch, J.M., Hewlett, J.D., 1982. A review of catchment experiments to determine the effect of vegetation changes on water yield and evapotranspiration. J. Hydrol. 55 (1–4), 3–23. https://doi.org/10.1016/0022-1694(82)90117-2.
- Bonan, G.B., 1999. Frost followed the plow: impacts of deforestation on the climate of the United States. Ecol. Appl. 9, 1305–1315. https://doi.org/10.1890/1051-0761(1999)009[1305:FFTPIO]2.0.CO, 2.
- Bouchez, J., Gaillardet, J., France-Lanord, C., Maurice, L., Dutra-Maia, P., 2011. Grain size control of river suspended sediment geochemistry: clues from Amazon River depth profiles. G-cubed 12. https://doi.org/10.1029/2010gc003380.
- Butler, B.M., Clay, R.B., Hargrave, M.L., Peterson, S.D., Schwegman, J.E., Schwegman, J.A., Welch, P.D., 2011. A new look at Kincaid: magnetic survey of a large Mississippian town. SE. Archaeol. 30 (1), 20–37.
- Citterio, A., Piégay, H., 2009. Overbank sedimentation rates in former channel lakes: characterization and control factors. Sedimentology 56, 461–482. https://doi.org/10.1111/j.1365-3091.2008.00979.x.
- Coleman, J.S.M., Rogers, J.C., 2003. Ohio River valley winter moisture conditions associated with the pacific—north American teleconnection pattern. J. Clim. 16 (6), 969—981.
- Commerford, J.L., Gittens, G., Gainforth, S., et al., 2022. Differences in forest composition following two periods of settlement by pre-Columbian Native Americans. Veg. Hist. Archaeobotany. https://doi.org/10.1007/s00334-021-00864-9
- Constantine, J.A., Dunne, T., Piégay, H., Kondolf, G.M., 2010. Controls on the alluviation of oxbow lakes by bed-material load along the Sacramento River, California. Sedimentology 57, 389–407. https://doi.org/10.1111/j.1365-3091.2009.01084.x.
- Counts, R.C., Murari, M.K., Owen, L.A., Mahan, S.A., Greenan, M., 2015. Late Quaternary chronostratigraphic framework of terraces and alluvium along the lower Ohio River, southwestern Indiana and western Kentucky, USA. Quat. Sci. Rev. 110, 72–91. https://doi.org/10.1016/j.quascirev.2014.11.011.
- Dai, A., 2013. The influence of the inter-decadal Pacific oscillation on US precipitation during 1923–2010. Clim. Dynam. 41, 633–646. https://doi.org/10.1007/s00382-012-1446-5.

- De Vries, J.L., Vrebos, B.A.R., 2002. Quantification of infinitely thick specimens by XRF analysis, In: van Grieken, R.E., Markovicz, A.A. (Eds.), Handbook of X-Ray Spectrometry, second ed. Marcel Dekker, New York, pp. 341-405.
- Dirmeyer, P.A., Kinter III., J.L., 2010. Floods over the U.S. Midwest: a regional water cycle perspective. J. Hydrometeorol. 11 (5), 1172–1181.
- Doperalski, M., 2017. Identification of a Middle Woodland period Mann phase hamlet: an archaeological investigation for a proposed development project in Posey County, Indiana. Indiana Archaeology 78.
- Dunne, T., Leopold, L.B., 1978. Water in Environ- Mental Planning. W. H. Free- man and Co, San Francisco.
- Easterling, D.R., Kunkel, K.E., Arnold, I.R., Knutson, T., LeGrande, A.N., Leung, L.R., Vose, R.S., Waliser, D.E., Wehner, M.F., 2017. Precipitation change in the United States. In: Wuebbles, D.J., Fahey, D.W., Hibbard, K.A., Dokken, D.J., Stewart, B.C., Maycock, T.K. (Eds.), Climate Science Special Report: Fourth National Climate Assessment, Volume I [Wuebbles. U.S. Global Change Research Program, Washington, DC, USA, pp. 207-230. https://doi.org/10.7930/J0H993CC.
- Fisk, H.N., 1947. Fine-Grained Alluvial Deposits and Their Effect on Mississippi River Activity: Vicksburg, Mississippi, U.S. Army Corps of Engineers, Mississippi River Commission, p. 82.
- Fisher, M.M., Brenner, M., Reddy, K.R., 1992. A simple, inexpensive piston corer for collecting undisturbed sediment/water interface profiles, 1992 J. Paleolimnol. 7, 157-161
- Gershunov, A., Barnett, T.P., 1998. Interdecadal modulation of ENSO teleconnections. Bull. Am. Meteorol. Soc. 79 (12), 2715-2726.
- Ghilardi, M., Kunesch, S., Styllas, M., Fouache, E., 2008. Reconstruction of Mid-Holocene sedimentary environments in the central part of the Thessaloniki Plain (Greece), based on microfaunal identification, magnetic susceptibility and grain-size analyses. Geomorphology 97 (3-4), 617-630.
- Graybeal, D.Y., Leathers, D.J., 2006. Snowmelt-related flood risk in appalachia: first estimates from a historical snow climatology. J. Appl. Meteorol. Climatol. 45 (1), 178-193
- Goodrich, G.B., Walker, J.M., 2011. The influence of the PDO on winter precipitation during high- and low-index ENSO conditions in the eastern United States. Phys. Geogr. 32 (4), 295-312. https://doi.org/10.2747/0272-3646.32.4.295.
- Greeley, W.B., 1925. The relation of geography to timber supply. Econ. Geogr. 1, 1–14. Haslett, J., Parnell, A., 2008. A simple monotone process with application to radiocarbon-dated depth chronologies. J. Roy. Stat. Soc.: Series C (Applied Statistics) 57, 399-418. https://doi.org/10.1111/j.1467-9876.2008.00623.
- Hatfield, J., 2012. Agriculture in the midwest. In: Winkler, J., Andresen, J., Hatfield, J., Bidwell, D., Brown, D. (Eds.), U.S. National Climate Assessment Midwest Technical Input Report, Coordinators. Available from the Great Lakes Integrated Sciences and Assessments (GLISA) Center. http://glisa.msu.edu/docs/NCA/ MTIT_Agriculture.pdf.
- Henderson, S.A., Vimont, D.J., Newman, M., 2020. The critical role of non-normality in partitioning tropical and extratropical contributions to PNA growth. J. Clim. 33 (14), 6273-6295.
- Higgins, S.A., Higgins, H.B., 2019. The Industrial Heritage of Lamasco. Cultural Resource Analysts, Inc. Indiana Dept. of Transportation.
- Horton, R., 1945. Erosional Development of Streams and Their Drainage Basins; Hydrophyical Approach to Quantitative Morphology, vols. 56-3. Geological Society of America Bulletin, pp. 275-370.
- Hu, Q., Feng, S., 2001. Variations of teleconnection of ENSO and interannual variation in summer rainfall in the Central United States. J. Clim. 14 (11), 2469–2480.
- Huang, Y., Tao, B., Xiaochen, Z., Yang, Y., Liang, L., Wang, L., Jacinthe, P.A., Tian, H., Ren, W., 2021. Conservation tillage increases corn and soybean water productivity across the Ohio River Basin. Agric. Water Manag. 254. https://doi.org/ 10.1016/j.agwat.2021.106962.
- ISEE Network, 2022. Soil explorer. Available at: http://SoilExplorer.net.
- Jenkins, R., 1999. Overview-XRF and XRD. Australian X-ray Analytical Association, Melbourne, VIC (Australia).
- Jonathan, M.P., Ram-Mohan, V., Srinivasalu, S., 2004. Geochemical variations of major and trace elements in recent sediments, off the Gulf of Mannar, the southeast coast of India. Environ. Geol. 45, 466-480. https://doi.org/10.1007/ s00254-003-0898-7
- Kessler, N.V., Welch, P.D., Butler, B.M., Brennan, T.K., Towner, R.H., Hodgins, G.W., 2022. Wiggle-matched red cedar from a pre-monumental occupation at Kincaid mounds, Illinois, USA. Tree-Ring Res. 78 (2), 100-112.
- King, K.W., Fausey, N.R., Williams, M.R., 2014. Effect of subsurface drainage on streamflow in an agricultural headwater watershed. Part A, Pages J. Hydrol. 519, 438-445. https://doi.org/10.1016/j.jhydrol.2014.07.035.
- Kluver, D., Leathers, D., 2015. Winter snowfall prediction in the United States using multiple discriminant analysis. Int. J. Climatol. 35 (8), 2003-2018. https:// doi.org/10.1002/joc.4103.
- Knox, J.C., 2000. Sensitivity of modern and Holocene floods to climate change. Quat. Sci. Rev. 19 (Issues 1-5), 439-457. https://doi.org/10.1016/S0277-3791(99)
- Knox, J.C., 1988. Climatic influence on upper Mississippi valley floods. In: Baker, V.R., Kochel, R.C., Patton, P.C. (Eds.), Flood Geomorphology. John Wiley & Sons, New York, pp. 279-300.
- Kunkel, K.E., Changnon, S.A., Angel, J.R., 1994. Climatic aspects of the 1993 upper Mississippi river basin flood. Bull. Am. Meteorol. Soc. 75 (5), 811–822.
- Lauer, J.W., Parker, G., 2008. Net local removal of floodplain sediment by river meander migration. Geomorphology 96 (1-2), 123-149.
- Lavers, D.A., Villarini, G., 2013. The nexus between atmospheric rivers and extreme precipitation across Europe. Geophys. Res. Lett. 40, 3259-3264. https://doi.org/

- 10.1002/grl.50636.
- Lapham, H.A., 2010. A baumer phase dog burial from the kincaid site in southern Illinois. Illinois Archaeology: Journal of the Illinois Archaeology Survey 22 (2).
- Leathers, D.J., Yarnal, B., Palecki, M.A., 1991. The pacific/north American teleconnection pattern and United States climate. Part I: regional temperature and precipitation associations. J. Clim. 4 (5), 517-528.
- Leigh, D.S., 2018. Vertical accretion sand proxies of gaged floods along the upper Little Tennessee River, Blue Ridge Mountains, USA. Sediment. Geol. 364, 342-350
- Leopold, L.B., 1994. A View of the River. Harvard University Press, Cambridge.
- Liu, Z., Yoshmura, K., Bowen, G.I., Welker, I.M., 2014. Pacific—north American teleconnection controls on precipitation isotopes (δ 180) across the contiguous United States and adjacent regions: a GCM-based analysis. J. Clim. 27 (3), 1046-1061
- Lintern, A., Leahy, P.J., Zawadzki, A., Gadd, P., Heijnis, H., Jacobsen, G., Connor, S., Deletic, A., McCarthy, D.T., 2016. Sediment cores as archives of historical changes in floodplain lake hydrology. Sci. Total Environ. 544, 1008-1019. https://doi.org/10.1016/i.scitotenv.2015.11.153.
- Livingstone, D.A., 1955. A lightweight piston sampler for lake deposits. Ecology 36 (1), 137-139. https://doi.org/10.2307/1931439.
- Lombardi, R., Davis, L., Therrell, M.D., 2021. Flood variability in the common era: a synthesis of sedimentary records from Europe and North America. Physical Geography, 1–15Mallakpour, I., Villarini, G. 2015. The changing nature of flooding across the central United States. Nat. Clim. Change 5, 250-254. https:// doi.org/10.1038/nclimate2516.
- Mallakpour, I., Villarini, G., 2015. The changing nature of flooding across the central United States. Nat. Clim. Change 5 (3), 250-254.
- Mann, M.E., et al., 2009. Global signatures and dynamical origins of the little Ice age
- and medieval climate anomaly. Science 326 (5957), 1256—1260.

 Mantua, N.J., Hare, S.R., Zhang, Y., Wallace, J.M., Francis, R.C., 1997. A pacific interdecadal climate oscillation with impacts on salmon production. Bull. Am. Meteorol. Soc. 78 (6), 1069-1080.
- Mills, C.M., Walsh, J.E., 2013. Seasonal variation and spatial patterns of the atmospheric component of the pacific decadal oscillation. J. Clim. 26 (5), 1575–1594.
- Mitsch, W., Day, J.W., 2006. Restoration of wetlands in the Mississippi-Ohio-Missouri (MOM) river basin: experience and needed research. Ecol. Eng. 26 (1), 55-69. https://doi.org/10.1016/j.ecoleng.2005.09.005.
- Muller, J., 2016. Late mississippian and historic. In: Archaeology of the Lower Ohio River Valley. Routledge, pp. 265-284.
- Munoz, S.E., Schroeder, S., Fike, D.A., Williams, J.W., 2014. A record of sustained prehistoric and historic land use from the Cahokia region, Illinois, USA, 2014 Geology 42 (6), 499-502.
- Munoz, S.E., Gruley, K.E., Massie, A., Fike, D.A., Schroeder, S., Williams, J.W., 2015. Cahokia's emergence and decline coincided with shifts of flood frequency on the Mississippi River. Proc. Natl. Acad. Sci. USA 112 (20), 6319-6324.
- Nakamura, J., Lall, U., Kushnir, Y., Robertson, A.W., Seager, R., 2013. Dynamical structure of extreme floods in the U.S. Midwest and the United Kingdom. J. Hydrometeorol. 14 (2), 485-504.
- Oliva, F., Viau, A.E., Bjornson, J., Desrochers, N., Bonneau, M.A., 2016. A 1300 year reconstruction of paleofloods using oxbow lake sediments in temperate southwestern Quebec, Canada. Can. J. Earth Sci. 53 (4), 378-386.
- Olsson, I., 1986. Radiometric methods. In: Berglund, B. (Ed.), Handbook of Holocene Palaeoecolgy and Palaeohydrology. John Wiley & Sons, Chichester, pp. 273–312.
- Page, B., Walker, R., 1991. From settlement to fordism: the agro-industrial revolution in the American midwest. Econ. Geogr. 67 (4), 281-315. https://doi.org/
- Pollard, H.J., 2020. Late Holocene Climate-Flood Relationships on the Lower Ohio River. Master's Thesis. Indiana University, Indianapolis, Indiana.
- Pompeani, D.P., Bird, B.W., Wilson, J.J., et al., 2021. Severe little Ice age drought in the midcontinental United States during the mississippian abandonment of cahokia. Sci. Rep. 11, 13829. https://doi.org/10.1038/s41598-021-92900-x.
- Pryor, S.C., Scavia, D., Downer, C., Gaden, M., Iverson, L., Nordstrom, R., Patz, J., Robertson, G.P., 2014. Ch. 18: midwest. In: Melillo, J.M., Terese, T.C., Richmond, Yohe, G.W. (Eds.), Climate Change Impacts in the United States: the Third National Climate Assessment. U.S. Global Change Research Program, pp. 418-440. https://doi.org/10.7930/J0J1012N.
- Pursell, C.C.O.B., 2016. Afterimages of Kincaid Mounds. Doctoral dissertation, Southern Illinois University, Carbondale, IL.
- Reimer, P., et al., 2020. The IntCal20 northern hemisphere radiocarbon age calibration curve (0-55 cal kBP). Radiocarbon 62 (4), 725-757. https://doi.org/ 10.1017/RDC.2020.41.
- Robinson, B.A., 2013. Regional bankfull-channel dimensions of non-urban wadeable streams in Indiana. Scientific Investigations Report 2013-5078.
- Rogers, J.C., Coleman, J.S.M., 2003. Interactions between the atlantic multidecadal oscillation, El Niño/La Niña, and the PNA in winter Mississippi valley stream flow. Geophys. Res. Lett. 30, 1518. https://doi.org/10.1029/2003GL017216,10.
- Schilling, K.E., Helmers, M., 2008. Effects of subsurface drainage tiles on streamflow in Iowa agricultural watersheds: exploratory hydrograph analysis. Hydrol. Process. 22, 4497–4506. https://doi.org/10.1002/hyp.7052.
- Schilling, K.E., Wolter, C.F., McLellan, E., 2015. Agro-hydrologic landscapes in the upper Mississippi and Ohio river basins. Environ. Manag. 55 (3), 646-656. https://doi.org/10.1007/s00267-014-0420-x.
- Schultz, R., Isenhart, T., Simpkins, W., et al., 2004. Riparian forest buffers in agroecosystems - lessons learned from the Bear Creek Watershed, central Iowa, 35-50. https://doi.org/10.1023/B: Agrofor. Syst. 61,

- AGFO.0000028988.67721, 4d.
- Serreze, M.C., Clark, M.P., McGinnis, D.L., Robinson, D.A., 1998. Characteristics of snowfall over the eastern half of the United States and relationships with principal modes of low-frequency atmospheric variability. J. Clim. 11 (2),
- Singh, S., Abebe, A., Srivastava, P., Chaubey, I., 2021. Effect of ENSO modulation by decadal and multi-decadal climatic oscillations on contiguous United States 36. Hydrol.: Reg. Stud. https://doi.org/10.1016/ streamflows. I. i.eirh.2021.100876.
- Smith, D.R., King, K.W., Johnson, L., Francesconi, W., Richards, P., Baker, D., Sharpley, A.N., 2015. Surface runoff and tile drainage transport of phosphorus in the midwestern United States, J. Environ, Qual. 44, 495–502. https://doi.org/ 10.2134/jeg2014.04.0176.
- Smith, A.B., Katz, R.W., 2013, US billion-dollar weather and climate disasters: data sources, trends, accuracy and biases. Nat. Hazards 67, 387-410. https://doi.org/ 10.1007/s11069-013-0566-5.
- Stafford, C.R., Creasman, S.D., 2002. The hidden record: late Holocene landscapes and settlement archaeology in the Lower Ohio River Valley. Geoarchaeology 17, 117-140. https://doi.org/10.1002/gea.10007.
- Strahler, A.N., 1957. Quantitative analysis of watershed geomorphology. Eos Trans.
- AGU 38 (6), 913—920. https://doi.org/10.1029/TR038i006p00913.
 Toonen, W.H.J., Kleinhans, M.G., Cohen, K.M., 2012. Sedimentary architecture of abandoned channel fills. Earth Surf. Process. Landforms 37, 459–472. https:// doi.org/10.1002/esp.3189.
- Toonen, W.H.J., Middelkoop, H., Konijnendijk, T.Y.M., Macklin, M.G., Cohen, K.M., 2016. The influence of hydroclimatic variability on flood frequency in the Lower Rhine. Earth Surf. Process. Landforms 41, 1266-1275.
- U.S. Geological Survey, 2020. National Water Information System Data Available on the World Wide Web. USGS Water Data for the Nation) accessed [June 10,

- 2020], at URL [http://waterdata.usgs.gov/nwis/.
- van Noordwijk, M., et al., 2017. Flood risk reduction and flow buffering as ecosystem services - Part 2: land use and rainfall intensity effects in Southeast Asia. Hydrol. Earth Syst. Sci. 21 (5), 2341-2360.
- Viau, A.E., Gajewski, K., Sawada, M.C., Fines, P., 2006. Millennial-scale temperature variations in north America during the Holocene. J. Geophys. Res. 111, D09102. https://doi.org/10.1029/2005JD006031.
- Wentworth, C.K., 1922. A scale of grade and class terms for clastic sediments. J. Geol. 30 (5) 377-392
- Wolman, M.G., Leopold, L.B., 1957. River flood plains: some observations on their formation. U. S. Geol. Surv. Prof. Pap. 282-C, 87-109.
- Wright, H.E., Mann, D.H., Glaser, P.H., 1984. Piston corers for peat and lake sediments. Ecology 65, 657–659.
- Wright, M.N., 2022. Late Holocene Climate-Flood Relationships on the White River. Indiana, USA. Master's Thesis. Indiana University, Indianapolis, Indiana.
- Xiao, Y., Wan, J., Hewings, G.J.D., 2013. Flooding and the midwest economy: assessing the midwest floods of 1993 and 2008. Geojournal 78, 245–258.
- Yim, W.W.S., Huang, G., Chan, L.S., 2004. Magnetic susceptibility study of Late Quaternary inner continental shelf sediments in the Hong Kong SAR, China. Quat. Int. 117-1, 41-54. https://doi.org/10.1016/S1040-6182(03)00115-0.
- Yu, B., Shabbar, A., Zwiers, F.W., 2007. The enhanced PNA-like climate response to pacific interannual and decadal variability. J. Clim. 20 (21), 5285–5300.
- Yu, B., Zwiers, F.W., 2007. The impact of combined ENSO and PDO on the PNA climate: a 1,000-year climate modeling study. Clim. Dynam. 29, 837-851. https://doi.org/10.1007/s00382-007-0267-4
- Zhang, W., Villarini, G., 2019. On the weather types that shape the precipitation patterns across the U.S. Midwest. Clim. Dynam. 53, 4217–4232. https://doi.org/ 10.1007/s00382-019-04783-4.